1963

Chromatographic measurement of gas-solid interaction potentials

James Anthony Murphy
Iowa State University

CHROMATOGRAPHIC MEASUREMENT OF GAS-SOLID INTERACTION POTENTIALS

by

James Anthony Murphy

A Dissertation Submitted to the
Graduate Faculty in Partial Fulfillment of
The Requirements for the Degree of
DOCTOR OF PHILOSOPHY

Major Subject: Physical Chemistry

Approved:

Signature was redacted for privacy.

In Charge of Major Work

Signature was redacted for privacy.

Head of Major Department

Signature was redacted for privacy.

Dean of Graduate College

Iowa State University
Of Science and Technology
Ames, Iowa

1963

TABLE OF CONTENTS

INTRODUCTION

Deviations of gases from ideality led early workers to realize that an attractive force existed between molecules. This led Eucken (1) in 1914 to attempt to explain the phenomenon of physical adsorption in terms of an attractive force between the gas molecules and the solid. He assumed that the gas in contact with a solid obeyed the Maxwell-Boltzman distribution law

$$C_x = C_\infty e^{-\mathcal{E}/RT} \tag{1}$$

where C_x is the concentration a distance x from the solid, C_∞ is the concentration in the gas phase, $\mathcal{E}$ is the potential, R is the gas constant and T is the absolute temperature. The number of moles adsorbed, v, is given by

$$v = AC_\infty x_o \int_{x_o}^{\infty} (e^{-\mathcal{E}/RT} - 1)\, dx \tag{2}$$

where A is the surface area and x_o the distance of closest approach of a molecule to the surface, taken to be the radius of an adsorbed molecule. The potential was assumed to be of the form

$$\mathcal{E} = -\frac{a x_o^m}{r^m} \tag{3}$$

Substitution of Equation 3 into Equation 2 results in

$$v = AC\, x_o \sum_{s=1}^{\infty} \frac{(a/RT)^s}{s!(ms-1)} \qquad (4)$$

In order to fit the data of nitrogen adsorbed on charcoal, Equation 4 was simplified by assuming a/RT to be large. The value of a was estimated from the combining law

$$a'_{12} = \sqrt{(a'_1 a'_2)}$$

where a'_1 and a'_2 are the boiling points of nitrogen and carbon respectively and a is approximately $3a'$. A satisfactory fit to the data was obtained with values of m, a, and Ax_o of 4, 2200, and -0.805 respectively. In 1922 (2) he extended this treatment to include a potential of the form

$$\varepsilon = -\frac{a_1}{x^m} + \frac{a_2}{x^n}$$

where m was chosen to be 4 and n to be 6. This model was more sucessful in fitting the experimental data.

Unfortunately the nature of the forces between molecules was unknown at this time and hence the values of the parameters were considered somewhat empirical.

Polanyi (3) on the other hand, avoided the necessity of choosing a specific form for the potential. His approach was to define the energy of adsorption of the ith phase, E_i, as the work necessary to remove a molecule from the ith phase to

the gas phase. Mathematically this is given by

$$E_i = \int_{\rho_g}^{\rho_i} V dP$$

where ρ_g is the density of the gas and ρ_i is the density of the ith phase. Since the equation of state of the adsorbed phase was unknown, it was assumed to be the same as the gas phase. A characteristic curve describing the dependence of the potential on the volume was calculated from experimental data and by assuming that the potential was independent of temperature, it was possible to determine the adsorption isotherm at any temperature.

However, in 1930 the nature of the forces between molecules possessing no permanent moment was understood. From second order perturbation theory, London (4) showed that the attractive potential due to dispersion forces was given by

$$\varepsilon(r) = -\frac{C_1}{r^6} - \frac{C_2}{r^8} - \frac{C_3}{r^{10}} - \cdots$$

where r is the distance between molecules. Methods for the evaluation of the constants C_i from theory have been summarized by Margenau (5), but none of these are in good agreement with ones obtained experimentally. However, they all predict that terms of order higher than C_2/r^8 are small and can be neglected with little error.

The advent of London's theory led many workers to attempt to calculate the heat of adsorption from theory alone. The total energy of interaction of a gas with a solid due to dispersion forces can be found by summing the potential over all molecules. Using an exponential repulsive term in r, Orr (6) was able to calculate the heat of adsorption of argon on both potassium chloride and cesium iodide by this method. However, the calculated value was 25 percent lower than the experimental one. Recently, however, Kiselev (7) has performed similar calculations with argon adsorbed on graphite. His agreement with experiment is within ten percent.

The above methods, however, are limited since the values of the constants must be known a priori and hence depend on formulae such as that developed by Kirkwood (8) and Müller (9). In addition, all of these calculations assume that there are no lateral interactions on the surface, but until 1954 most of the experimental data was obtained in a region below the critical temperature of the gas and at appreciable coverages and hence the comparison of the calculated with experimental values of the heat of adsorption is of questionable value.

Steele and Halsey (10) on the other hand obtained very accurate data at low pressures and temperatures well above the critical temperature. In this case the principal contribution is the adsorption of single atoms on the surface. For their data they were able to show that

$$V_a - V_{geo} = \int_{V_{geo}} (e^{-\ /kT} - 1)dV \tag{5}$$

where V_a is the apparent volume of the system and V_{geo} is the geometric volume of the system. The Sutherland model was assumed for the potential and instead of summing the potential over all atoms, the distance of a gas molecule from the surface was assumed to be large compared to the distance of nearest neighbors in the solid and hence the summation may be replaced by integration. The potential then became

$$\mathcal{E}(x) = \rho \int_0^{2\pi} d\phi \int_0^{\pi/2} \sin\theta d\theta \int_{\frac{x}{\cos\theta}}^{\infty} \mathcal{E}(r) r^2 dr \tag{6}$$

where ρ is the density of the solid and x is the distance of the gas molecule from the surface. Substitution of $\mathcal{E}(x)$ into Equation 5 yields

$$V_a - V_{geo} = AD \sum_{n=0}^{\infty} \frac{(\mathcal{E}_o/kT)^n}{n!(3n-1)} \tag{7}$$

where D is the distance of the molecule from the surface at the potential minimum $\mathcal{E}_o$ and A is the surface area. They were able to obtain reasonable values of the parameters AD and

ε_o by fitting their data to Equation 7. There was no way to separate the parameters A and D within the framework of the theory and hence they chose to evaluate D and hence A by the Kirkwood-Müller formula. The surface area obtained in this way was smaller than by the BET method, but considering the simplicity of the model the agreement was good. For a given solid the calculated areas were less, the larger the adsorbate molecule.

The success of this treatment led DeMarcus, Hopper and Allen (11) and Freeman (12) to extend this treatment to the more realistic Lennard-Jones 12-6 potential. This potential was integrated over the solid according to Equation 6 and substituted into Equation 5. The integration was performed numerically to obtain a theoretical curve of $\ln(V_a-V_{geo})/Ax_o$ as a function ε_o/kT. They found that the experimental data fit this model better than the original model of Steele and Halsey (10).

In 1959 Hansen (13) attacked the problem in a similar manner. He showed that Equation 5 is exact for the limiting case of zero pressure and evaluated it analytically for the Lennard-Jones 12-6 potential to obtain

$$\lim_{P\to 0}\left(\frac{NkT}{P} - V\right) = \frac{1}{9}\left(\frac{2}{15}\right)^{1/6}\mu^{1/9}\, A\sigma \sum_{n=0}^{\infty} \frac{\mu^{2n/3}}{n!}\,\Gamma\left(\frac{3n-1}{9}\right)$$

where 0.3849μ is equal to ε_o and $(2/15)^{1/6}\sigma$ is equal to x_o.

He also pointed out that the value of x_o may be found from the van der Waals radii of the adsorbent and adsorbate and the combining laws of Hirschfelder, Curtiss and Bird (14).

Since this time Halsey and coworkers have improved their experimental apparatus (15). More accurate data has been obtained for the rare gases on a graphitized carbon (16) and with this they have tried to find the exact form of the potential. This has met with some success. They have also tried to extend the treatment to account for lateral interactions on the surface (17), but this has met with little success.

Hanlan and Freeman (18) have interpreted data obtained from gas adsorption chromatography by the Halsey theory and the results looked promising. They measured the difference between the retention volume of a series of hydrocarbons and that of hydrogen as a function of temperature. By assuming both hydrogen and the carrier gas helium to be ideal, they were able to equate this difference to the quantity V_{ex} defined by Halsey. The data fit this model quite well and the values of the parameters obtained seemed reasonable. Although the reproducibility of the parameters was not tested, their work indicates that chromatographic data may be used to study gas-solid interactions.

EXPERIMENTAL

The chromatograph used in these experiments was essentially a Research Specialties Company 600 series gas chromatograph. It consisted of a Model 604 Main Control Unit, Model 605-1 Katharometer Power Supply, Model 606 Flow Controller, Model 607-3 Proportional Temperature Controller and a Model 608-1 Recorder Unit. The recorder was a Leeds and Northrup Speedomax H recorder with a nine inch chart and a one-half inch per minute chart speed. The remaining components were constructed at this laboratory.

Since precise temperature was desired, a constant temperature bath was constructed rather than an oven as is employed in most chromatographs. The bath was designed to operate in the temperature range of 25°C to 500°C with a temperature fluctuation of less than 0.05°C over the entire range.

The bath consisted of a stainless steel tank, ten inches high by nine inches in diameter with a one inch transite top. The tank rested on a three-eighths inch copper plate heated by a 1500 watt ring heater controlled by a variable transformer. Surrounding this tank was another heater separated from the bath by one-fourth inch of insulation and controlled by a separate variable transformer. A third heater was inserted directly into the bath and controlled by the proportional temperature controller which uses a platinum resistance thermometer as its sensing element. The heater and thermometer

were placed as close as possible to minimize fluctuations caused by a thermal lag.

The bath was inserted into a metal box lined with fire brick and insulated with Zonolite. With this system it was possible to maintain the temperature to within 0.05°C over the period of one run.

The temperature of the bath was measured with a platinum resistance thermometer and a Mueller Bridge calibrated by the National Bureau of Standards. The null point was determined with a Leeds and Northrup D.C..Guarded Null Detector (No. 9834). With this instrumentation a change in temperature of 0.001°C was easily observed.

The flow type katharometer detector, shown in Figure 1, was constructed from a piece of stainless steel one and five-eighths inch in length and two inches in diameter. It was designed to withstand immersion in a fused salt (sodium nitrite-potassium nitrate eutectic) bath up to a temperature of 500°C. The accuracy with which the dependence of the retention time on temperature was desired, necessitated the incorporation of certain features into the design of the detector. Three of these features were:

1. A signal is recorded on both the reference and sensing sides of the detector. A large negative signal is generated on the reference side and a positive signal, the usual chromatographic peak,

Figure 1. Katharometer Detector

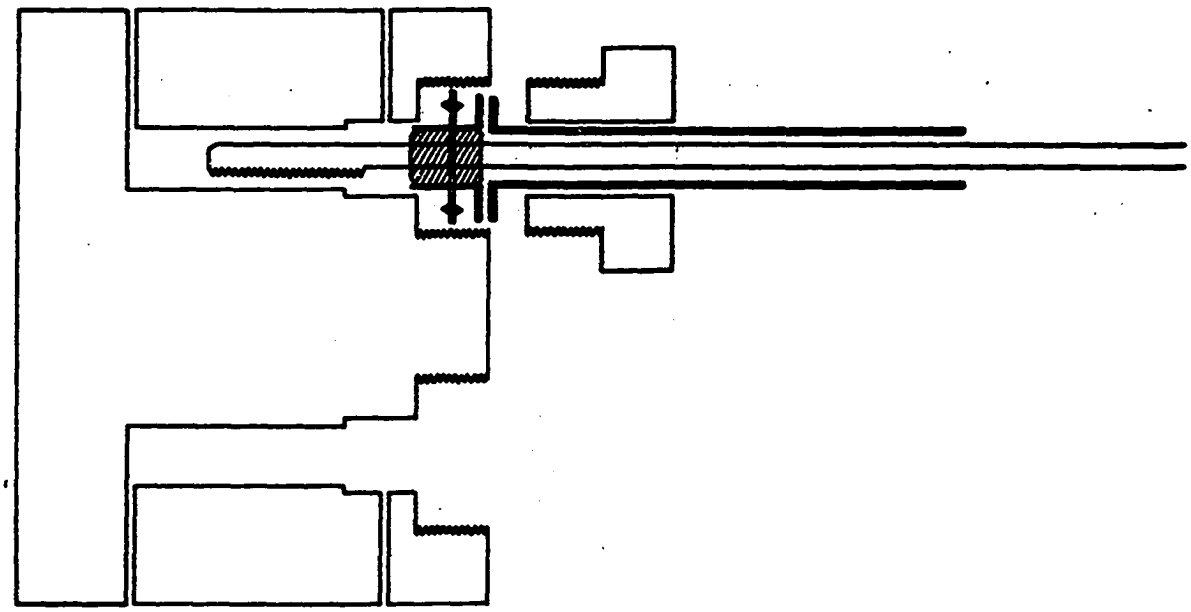

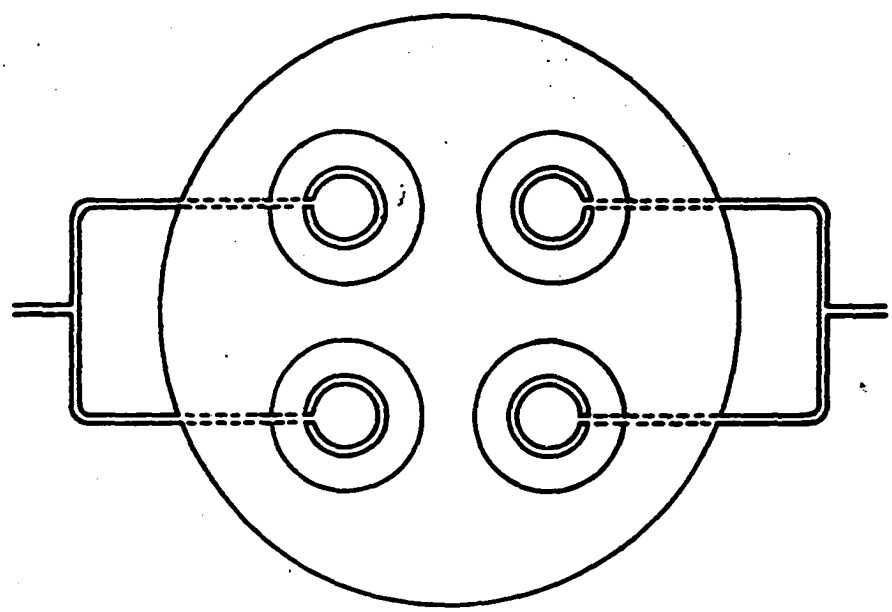

on the sensing side (Figure 2). The retention time, uncorrected for dead space, is then the distance between the two peak maxima multiplied by the recorder chart speed.

2. The gas stream is split before it passes over the filaments into two equal streams, each of which passes over but one filament. This ensures that the peak maximum denotes the maximum concentration of gas.

3. The electrical leads emerge from the top of the detector. This facilitates their insulation from an electrical conducting bath medium, such as a fused salt.

The filaments employed in the detector were Type W 9225 tungsten filaments obtained from Gow Mac Instrument Company. The gas-tight seal was accomplished by means of a double knife edge washer (19). One of these washers was placed in each of the filament wells. On top of these were placed one filament and a flared, one-quarter inch stainless steel tube. The seal was made by tightening with a box wrench a one-half inch hexagonal nut with a half-twenty thread.

The flow meter was a 22 millimeter glass tube whose volume was calibrated with mercury. The flow rate was the time required for a film of sodium laurylsulfate to traverse

Figure 2. Typical Chromatogram

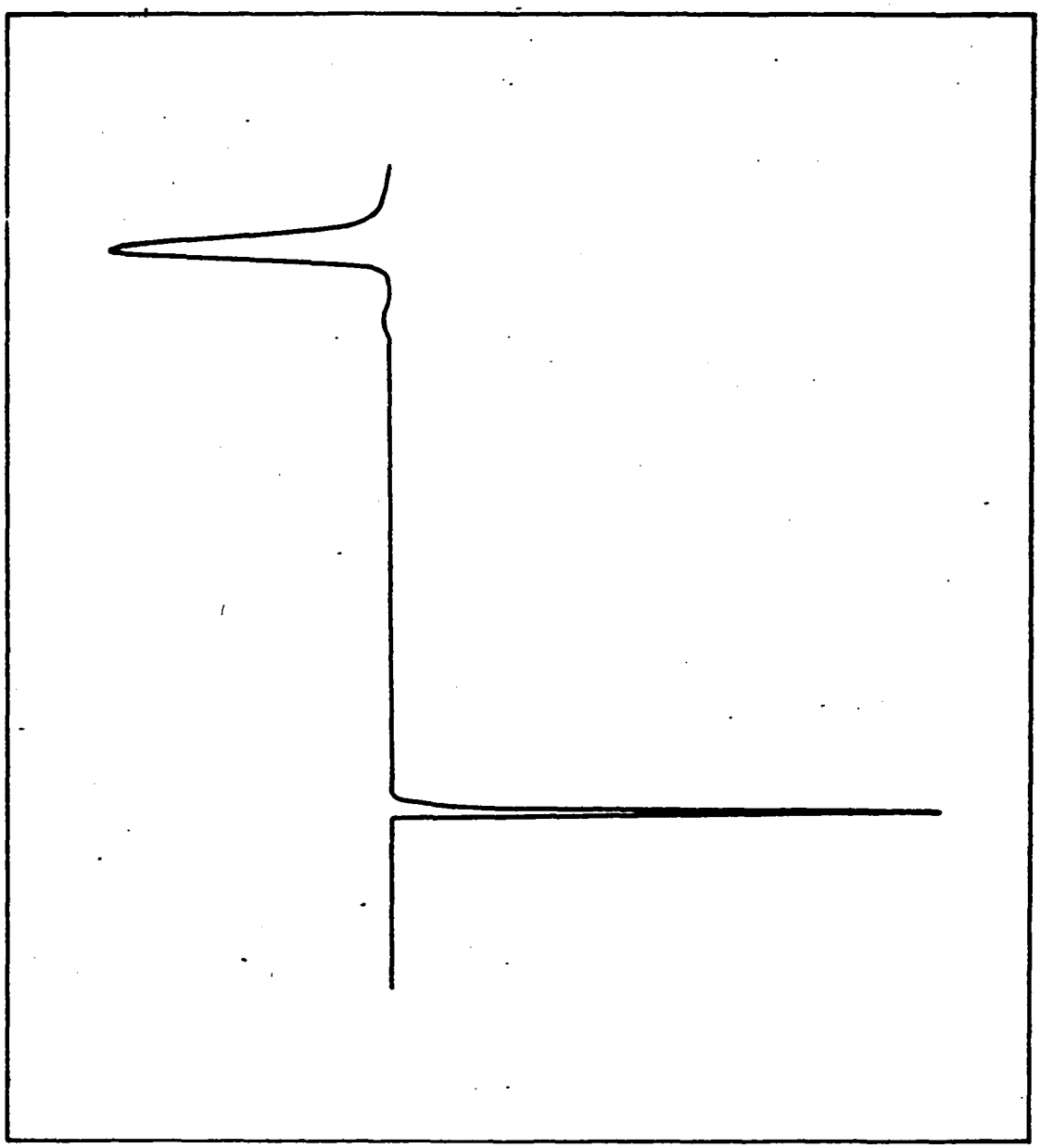

the known volume.

The pressure gradient across the column was measured with a mercury manometer.

The gas sampling device was a Gas Sample Valve (No. 154-0067) obtained from Perkin-Elmer Company. The sample volume used in all of the experiments was 0.10 cc.

The bath medium in the temperature range 25°C to 150°C was mineral oil. In the temperature range 150°C to 500°C, it was replaced with a sodium nitrite-potassium nitrate eutectic mixture. The mixture was circulated by a stirrer with a three inch blade.

A schematic diagram of the actual experiment is given in Figure 3. The carrier gas, helium, passes from a cylinder where the flow rate is adjusted. From here it enters the gas sampling valve where the sample can be introduced. The gas sample and/or carrier gas is split into two equal streams each of which passes over one filament on the reference side of the detector. This produces a sharp negative signal. The two streams are then rejoined and pass through the packed column. After passing through the column, the stream is again split into two equal streams each of which passes over one filament on the sensing side. This produces a positive signal which is the standard chromatographic peak. The gas then passes through the flow meter into the atmosphere.

The substrate used in all of these experiments was

Figure 3. Schematic Diagram of apparatus

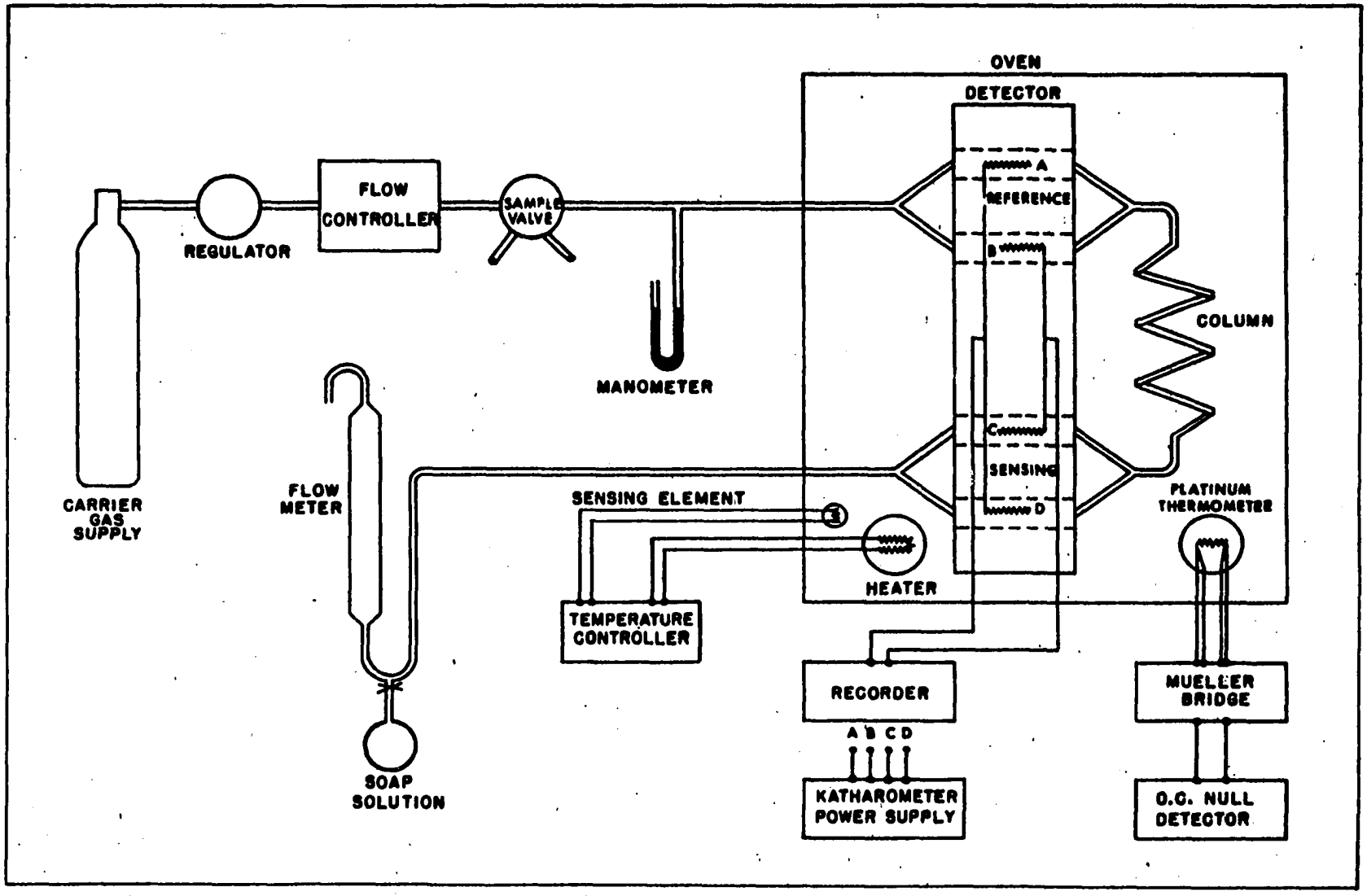
OVEN
DETECTOR
A
REFERENCE
B
COLUMN
C
SENSING
D
FLOW CONTROLLER
SAMPLE VALVE
REGULATOR
MANOMETER
CARRIER GAS SUPPLY
FLOW METER
SENSING ELEMENT
PLATINUM THERMOMETER
HEATER
TEMPERATURE CONTROLLER
RECORDER
MUELLER BRIDGE
A B C D
KATHAROMETER POWER SUPPLY
D.C. NULL DETECTOR
SOAP SOLUTION

"Columbia L" activated charcoal obtained from National Carbon Company. This was sieved to exclude particles larger than 20 mesh and smaller than 40 mesh. Before packing the column, it was heated at 500°C under a vacuum of 0.001 mm. of mercury for two days. This was then packed into a one-quarter inch stainless steel tube and coiled into a spiral of five inches in diameter. The substrate did not change weight from the beginning of the experiment to its completion, a period of approximately two weeks. This indicates that little, if any, of the carbon was oxidized.

Neon was chosen as the marker gas since it is closer to ideality than any other gas with the exception of helium which was used as the carrier gas. Hydrogen was also considered since it is close to ideality and has an added advantage of lower cost. However, it proved to be unsuitable in these experiments since concentrations greater than 12 mole percent gave complex peaks and resulted in large errors in the measurement of the retention time. The explanation of these complex peaks is given in Appendix A.

THEORY

The phenomenon of physical adsorption can be treated by the method of statistical mechanics in a manner analogous to the treatment of imperfect gases (20). The classical partition function, Z, of a gas consisting of N molecules in contact with a surface of area A is given by

$$Z = \frac{2\pi mkT}{h^2}^{3/2\ N} Q_I^N \frac{1}{N!} \int \cdots \int e^{-W/kT} dV_1 \cdots dV_N \qquad (8)$$

where Q_I is the partition function for the internal degrees of freedom and W is the potential energy of the entire system. If at this point the simultaneous interaction of a molecule with more than one other is neglected, the W is given by

$$W = \sum_i \sum_{j>i} \mathcal{E}(r_{ij}) + \sum_k \mathcal{E}(r_{ks}) \qquad (9)$$

where $\mathcal{E}(r_{ij})$ is the potential between the ith and jth atoms in the gas phase separated by a distance r_{ij} and $\mathcal{E}(r_{ks})$ is the distance between the kth gas atom and the surface separated by a distance r_{ks}. If there are p pairs of molecules and m surface interactions, substitution of Equation 9 into Equation 8 and performing the integrations yields

$$Z = \left(\frac{2\pi mkT}{h^2}\right)^{3/2\ N} Q_I^N \frac{V^N}{N!} \sum_{m=0}^{N} \sum_{p=0}^{\frac{N-m}{2}} \frac{N! \left(\frac{2B}{V}\right)^p \left(\frac{\beta A}{V}\right)^m}{m!p!(N-2p-m)!2^p} \tag{10}$$

defining

$$-B = 1/2 \int_o^\infty \left(e^{-\mathcal{E}(r_{ij})/kT} - 1\right) 4\pi r_{ij}^2 \, dr_{ij} \tag{11}$$

the second virial coefficient of the gas and

$$-\beta A = A \int_o^\infty \left(e^{-\mathcal{E}(z)/kT} - 1\right) \, dz \tag{12}$$

where z is the distance of the gas molecule from the surface. For p and m small and hence for leading terms

$$(N - 2p - m)! \cong (N - m - p)!$$

Furthermore if the series is sufficiently rapid in convergence, it is immaterial whether the sum is carried to $\frac{N - m}{2}$ or to N - m. With these approximations Equation 10 becomes

$$Z = \left(\frac{2\pi mkT}{h^2}\right)^{3/2\ N} Q_I^N \frac{(V - NB - \beta A)^N}{N!} \tag{13}$$

Equation 12 is exact only in the case of zero pressure. In this case B is zero and Equation 13 becomes exactly

$$Z = \left(\frac{2\pi mkT}{h^2}\right)^{3/2\ N} Q_I^N \frac{(V - \beta A)^N}{N!} \tag{14}$$

If Q_I is assumed to be independent of volume and use is made of the Sterling approximation and the relationship between the free energy and the partition function, then Equation 14 becomes

$$\lim_{p \to 0} \left(\frac{NkT}{p} - V\right) = -\beta A \tag{15}$$

Equation 15 is exact as it stands and hence is the equation of state for a gas in contact with a surface in the limiting case of zero pressure. In order to proceed further, the dependence of the potential on distance must be known. Since the Lennard-Jones potential is adequate for the explanation of gas-gas interactions, it seems reasonable to assume it will also be satisfactory for gas-solid interactions. The general form of this potential is

$$(r) = -\frac{\alpha}{r^p} + \frac{\beta}{r^q}$$

In general this potential should be summed over all atoms in the solid, but in the case that the distance between the gas and the solid is large compared with the distance between closest neighbors in the solid, then the summation may be

replaced by integration to yield

$$\mathcal{E}(z) = \mathcal{E}(z_o)\left[\frac{m}{m-n}\left(\frac{z_o}{z}\right)^n - \frac{n}{m-n}\left(\frac{z_o}{z}\right)^m\right] \tag{16}$$

where z_o is the distance of the gas molecule from the surface at the potential minimum $\mathcal{E}(z_o)$, n is p - 3, and m is q - 3. Substitution of Equation 16 into Equation 12 yields

$$-\frac{\beta A}{A z_o} = \left(\frac{nt}{m-n}\right)^{\frac{1}{m}} \sum_{k=0}^{\infty} \frac{\left[\left(\frac{m}{n}\right)^{\frac{n}{m}} \left(\frac{mt}{m-n}\right)^{\frac{m-n}{m}}\right]^k \Gamma\left(\frac{nk+m-1}{m}\right)}{k!(nk-1)} \tag{17}$$

where $t = -\mathcal{E}(z_o)/kT$. Equation 17 converges for all values of $t > 0$, but its convergence is slow for large t. Hence, this equation has been evaluated for the cases m = 9, n = 3 and $m = \infty$, n = 3 (Appendix B). The $\ln(-\beta A/Az_o)$ has been graphed as a function of t for both of these models and is given in Figure 4. Examination of this graph reveals that the curve is almost linear for $t > 4$. This is the range of most experimental data. Hence an asymptotic expansion valid for large t was developed for convenience in evaluating the data and for a more thorough understanding of the evaluation of the parameters. For this purpose, we assume that $-\mathcal{E}(z)/kT$ has a unique maximum at $z = z_o$ and let

$$-\mathcal{E}(z) = t(1 - h(x))$$

Figure 4. Theoretical curves for gas-solid interactions

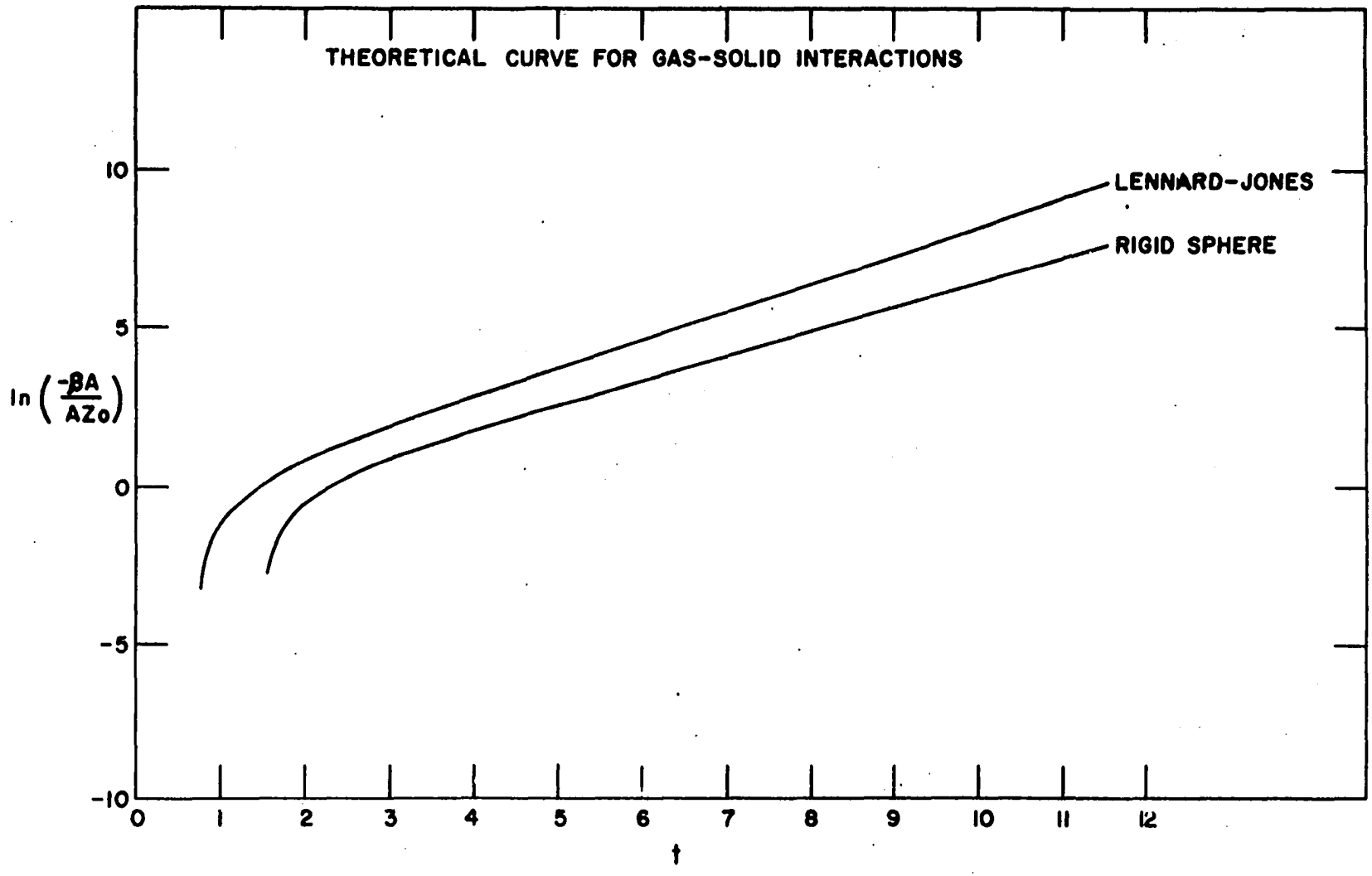
THEORETICAL CURVE FOR GAS-SOLID INTERACTIONS
LENNARD-JONES
RIGID SPHERE
10
5
0
-5
-10
$\ln\left(\frac{-\beta A}{AZ_0}\right)$
0
1
2
3
4
5
6
7
8
9
10
11
12
t

where $x = z/z_o$. Equation 12 then becomes

$$-\beta A = Az_o t^{-1/2} e^t G(t) \tag{18}$$

where

$$G(t) = \int_o^\infty t^{1/2} \left[e^{-th} - e^{-t} \right] dx \tag{19}$$

It will be convenient to consider G(t) as a sum of terms as follows

$$G(t) = \int_{1-y}^{1+y} t^{1/2} e^{-th} dx - (1+y)e^{-t} + \int_o^{1-y} t^{1/2} e^{-th} dx$$

$$+ \int_{1+y}^\infty t^{1/2} (e^{-th} - e^{-t}) \, dx \tag{20}$$

We shall expect to choose y in the range $0 < y < 1$, so that the first term on the right is the principal contribution to G(t). Let $u = x - 1$, then

$$\int_{1-y}^{1+y} t^{1/2} \, e^{-th(x)} dx = \int_{-y}^{y} t^{1/2} \, e^{-th(u)} du \tag{21}$$

Now h(u) has a unique minimum at $u = 0$, and since $\mathcal{E}(z)$ has no singularities for $z > 0$, we have

$$h(u) = \sum_{n=2}^{\infty} \frac{h_o^{(n)}}{n!} u^n \tag{22}$$

where $h_o^{(n)}$ is the nth derivative of h with respect to u evaluated at u = 0, and the series is absolutely convergent for $|u| \leq y < 1$. In this same range

$$e^{-th} = e^{-1/2\ th_o^{(2)}\ u^2} \sum_{m=0}^{\infty} \frac{(-1)^m t^m}{m!} \left[\sum_{n=3}^{\infty} \frac{h_o^{(n)}}{n!} u^n \right]^m \tag{23}$$

Let $a_n = h_o^{(n+3)}/(n+3)!$, then Equation 23 becomes

$$e^{-th} = e^{-1/2\ th_o^{(2)}\ u^2} \sum_{m=0}^{\infty} \sum_{n=0}^{\infty} (-1)^m t^m u^{n+3m} (\Sigma\Pi) \frac{a_i^{n_i}}{n_i!} \tag{24}$$

where the operator $(\Sigma\Pi)$ denotes the sum of all products of terms $a_i^{n_i}/n_i!$ such that $\Sigma n_i = m$, $\Sigma i n_i = n$. Substitution of 24 into 21 yields

$$\int_{-y}^{y} t^{1/2}\ e^{-th} du = \sum_{m=0}^{\infty} \sum_{n=0}^{\infty} (-1)^m t^{m + 1/2} (\Sigma\Pi) \frac{a_i^{n_i}}{n_i!}$$

$$\int_{y}^{y} u^{n+3m}\ e^{-1/2\ th_o^{(2)}\ u^2}\ du \tag{25}$$

Now if n + 3m is odd, the integral on the right hand side of Equation 25 is zero. If n + 3m is even, then n + m is also even. Let n + m = 2p, n + 3m = 2(p + m), then

$$\int_{-y}^{y} u^{2p+2m_e - 1/2}\, th_o^{(2)} u^2\, du = \Gamma(p+m+1/2)\left[\frac{2}{th_o^{(2)}}\right]^{p+m+1/2}$$

$$\left\{erf\left[y\left(\frac{1}{2}th_o^{(2)}\right)1/2\right] - e^{-1/2\, th_o^{(2)} y^2} \sum_{k=0}^{p+m} \frac{\left(\frac{1}{2}th_o^{(2)} y^2\right)^{k-1/2}}{\Gamma(k+1/2)}\right\} \tag{26}$$

or using an asymptotic form for erf x valid for large x, this becomes

$$\int_{-y}^{y} u^{2p+2m_e - 1/2}\, th_o^{(2)} u^2\, du = \Gamma(p+m+1/2)\left[\frac{2}{th_o^{(2)}}\right]^{p+m+1/2} \left\{1 - e^{-1/2\, th_o^{(2)} y^2}\left[\sum_{k=1}^{p+m} \frac{\left(\frac{1}{2}th_o^{(2)} y^2\right)^{k-1/2}}{\Gamma(k+1/2)} + \sum_{k=0}^{q} \frac{\Gamma(1/2-k)}{\pi}\left(\frac{1}{2}th_o^{(2)} y^2\right)^{-k-1/2}\right]\right\} \tag{27}$$

where the second series may be terminated at its least term

or earlier if convenient. Substituting 27 into 25 and rearranging the series gives

$$\int_{-y}^{y} t^{1/2}\, e^{-th}\, du = \left(\frac{2}{h_o^{(2)}}\right)^{1/2} \sum_{p=0}^{\infty} \left(\frac{2}{th_o^{(2)}}\right)^{p}$$

$$\sum_{m=0}^{2p} (-1)^m \left(\frac{2}{h_o^{(2)}}\right)^{m} \Gamma(p+m+1/2)\,(\Sigma\pi)' \frac{a_i^{n_i}}{n_i!} \left[1-e^{-1/2\, th_o^{(2)} y^2}\right.$$

$$\left. \left\{ \sum_{k=1}^{p+m} \frac{\left(\frac{1}{2} th_o^{(2)} y^2\right)^{k-1/2}}{\Gamma(k+1/2)} + \sum_{k=0}^{q} \frac{\Gamma(1/2-k)}{\pi (1/2\, h_o^{(2)} y^2)^{k+1/2}} \right\} \right] \tag{28}$$

where $(\Sigma\pi)'$ denotes the sum of all products of terms $a_i^{n_i}/n_i!$ such that $\Sigma n_i = m$, $\Sigma i n_i = 2p - m$.

Defining

$$b_i = \frac{2}{h_o^{(2)}}\, a_i = \frac{2}{(i+3)!}\, \frac{h_o^{(i+3)}}{h_o^{(2)}}$$

gives

$$\int_{-y}^{y} t^{1/2} e^{-th}\, du = \left(\frac{2}{h_o^{(2)}}\right)^{1/2} \sum_{p=0}^{\infty} \left(\frac{2}{th_o^{(2)}}\right)^{p}$$

$$\sum_{m=0}^{2p} (-1)^m \Gamma(p+m+1/2)(\Sigma\pi)' \frac{b_i^{n_i}}{n_i!} \left[1 - e^{-1/2\ th_o^{(2)} y^2} \right.$$

$$\left. \left\{ \sum_{k=1}^{p+m} \frac{\left(\frac{1}{2} th_o^{(2)} y^2\right)^{k-1/2}}{\Gamma(k+1/2)} + \sum_{k=0}^{q} \frac{\Gamma(1/2-k)}{\pi(\frac{1}{2} th_o^{(2)} y^2)^{k+1/2}} \right\} \right]$$

(29)

It should be noted that from its derivation, the term involving $e^{-1/2\ th_o^{(2)} y^2}$ for fixed p and m is positive and less than one, and for $th_o^{(2)} y^2$ large, p small this term must be small and of order $(1/2\ th_o^{(2)} y^2)^{3p}\ e^{-1/2\ th_o^{(2)} y^2}$ at most. Only such terms in the series will prove useful and it will be practical to choose y sufficiently close to one that it may be replaced by one in such terms with negligible physical error.

The second term on the right hand side of Equation 20 is small for large t and y~1 and can be neglected. The third term can be bounded in the following manner.

$$\int_0^{1-y} t^{1/2}\ e^{-th}\ dx \leq (1-y)\ t^{1/2}\ e^{-th(-y)}$$

(30)

For common potentials $h(-1) \to \infty$ and hence this term can be

made arbitrarily small by choosing y sufficiently close to one. The last term is treated in the following manner.

$$\int_{1+y}^{\infty} t^{1/2}(e^{-th}-e^{-t})dx \leq (b-1-y)\ t^{1/2}(e^{-th}-e^{-t}) +$$

$$t^{1/2}\ e^{-t} \int_{b}^{\infty} e^{t(1-h)}dx \tag{31}$$

Hence for large t, a suitable representation for G(t) is given by

$$G(t) \cong \left(\frac{2}{h_o^{(2)}}\right)^{1/2} \sum_{p=0}^{n} \left(\frac{2}{th_o^{(2)}}\right)^{p} \sum_{m=0}^{2p} (-1)^m \Gamma(p+m+1/2)(\Sigma\pi)' \frac{b_i^{n_i}}{n_i!}$$

$$\left[1 - O\left\{\left(\tfrac{1}{2}th_o^{(2)}\right)^{p+m} e^{-1/2\ th_o^{(2)}}\right\}\right] +$$

$$t^{1/2}\ e^{-t}\left[\int_{2}^{\infty}\left(e^{t(1-h)}-1\right)\ dx - 2\right] \tag{32}$$

The error in this representation is of the order of the (n + 1)st term in the series. O(x) means a term of order of magnitude x. The integral can be evaluated approximately or bounded. If we denote S_n by

$$S_n = \left(\frac{2}{h_o^{(2)}}\right)^{1/2} \sum_{p=0}^{n} \left(\frac{2}{th_o^{(2)}}\right)^{p} \sum_{m=0}^{2p} (-1)^m \Gamma(p+m+1/2)(\Sigma\Pi)' \frac{b_i^{n_i}}{n_i!} \qquad (33)$$

then

$$\lim_{t\to\infty} t^n \left[G(t) - S_n\right] = 0$$

and hence this series is an asymptotic representation of G(t). Now from Equations 18, 32 and 33, a representation of the problem is given by

$$-\frac{\beta A}{Az_o} = t^{-1/2} e^t S_n + R(t) \qquad (34)$$

If the potential is given by

$$-\frac{\mathcal{E}(x)}{kT} = t\left(\frac{m}{m-n} x^{-n} - \frac{n}{m-n} x^{-m}\right) \qquad (35)$$

then

$$h(u) = 1 - \frac{m}{m-n}(1+u)^{-n} + \frac{n}{m-n}(1+u)^{-m}$$

$$h_o^{(k)} = (-1)^k \frac{mn}{m-n}\left[\frac{(m+k-1)!}{m!} - \frac{(n+k-1)!}{n!}\right]$$

$$b_i = -\frac{2(-1)^i}{(i+3)!(m-n)}\left[\frac{(m+i+2)!}{m!} - \frac{(n+i+2)!}{n!}\right]$$

For the case of m = 9, n = 3, Equation 34 becomes

$$-\frac{\beta A}{Az_c} = t^{-1/2} e^t \left(\frac{2\pi}{h_o^{(2)}}\right)^{1/2} \left[1 + \frac{175}{216t} + \frac{140105}{93312t^2} + R'(t)\right] \qquad (36a)$$

or to about the same approximation

$$\ln(-\beta A t^{1/2}/Az_o) \cong t + 1/2 \ln(2\pi/h_o^{(2)}) + \frac{175}{216t} +$$

$$\left[\frac{140105}{93312t^2} - \frac{1}{2}\ \frac{175}{216}\right] \frac{1}{t^2} + R'' \qquad (36b)$$

Comparison of Equation 36a with 17 has been performed and the difference between the logarithms of these equations neglecting R'(t) is given in Table 1. It can be seen that a fortuitous cancellation of errors is responsible for the fit to t = 3. If not for this cancellation of errors, the range of validity of Equation 36a would be $t > 7$.

It is clear from Equations 33 and 34 that the curve of $\ln\left(-\frac{\beta A}{Az_o} t^{1/2}\right)$ as a function of t is linear for large t. Hence, if one plots $\ln(-\beta A T^{-1/2})$ versus 1/T, the limiting slope for small T is $\varepsilon(z_o)/R$. Clearly then, the depth of the potential well can be unambiguously determined. $\varepsilon(z_o)$ can be related to the energy of adsorption in a simple way.

The excess energy of the gas due to interaction with the solid, in the limit as $C_o \to 0$, is

$$E = \int_0^\infty C(z)\,\mathcal{E}(z)\,dz = C_o \int_0^\infty \mathcal{E}(z) e^{-\mathcal{E}(z)/kT} dz \tag{37}$$

The surface excess in this limit is

$$\Gamma = C_o \int_0^\infty (e^{-\mathcal{E}(z)/kT} - 1)\,dz \tag{38}$$

Table 1. Comparison of Equations 17 and 36 for 9-3 potential

t	Equation 17 $\ln(-\beta A/Ax_o)$	Equation 36 $\ln(-\beta A/Ax_o)$	Difference
0.76980	-3.21309	1.6949	-4.9080
0.96225	-1.41799	1.4976	-2.9156
1.15470	-0.63544	1.3929	-2.0283
1.34715	-0.15351	1.3566	-1.5101
1.53960	0.20911	1.3648	-1.1557
1.73205	0.50810	1.4055	-0.8974
1.92450	0.76810	1.4705	-0.7024
2.11695	1.00214	1.5544	-0.5523
2.30940	1.21810	1.6522	-0.4341
3.07920	1.98086	2.1396	-0.1587
3.84900	2.67194	2.7175	-0.0456
4.61880	3.34344	3.3445	-0.0011
5.38860	4.01520	4.0015	0.0137
6.15840	4.69461	4.6936	0.0010
6.92820	5.38367	5.3696	0.0141
7.69800	6.08209	6.0710	0.0111
8.46780	6.78872	6.7810	0.0077
9.23760	7.50229	7.4971	0.0052
10.00740	8.22150	8.2183	0.0032
10.77720	8.94566	8.9439	0.0018
11.54700	9.67360	9.6730	0.0006

Therefore the excess energy per mole surface excess is

$$\frac{E}{\Gamma} = \frac{d \ln(\lim_{C_o \to 0} \Gamma/C_o)}{d(1/kT)} = \frac{d \ln(-\beta A)}{d(1/kT)} \qquad (39)$$

Combining this expression with Equation 36b yields

$$\frac{E}{\Gamma} = \mathcal{E}(z_o)\left[1 - \frac{1}{2t} - \frac{175}{216t} - \frac{140105}{93312t^2}\right] + R'''(t) \qquad (40)$$

Clearly then, $\mathcal{E}(z_o)$ is the excess energy when determined for large t. This is equivalent to the energy of adsorption at absolute zero, i.e. all molecules are in their ground state.

If one extrapolates the limiting slope to t = 0, then the intercept will be given by

$$\ln\left[Az_o\left(\frac{2\pi}{h_o^{(2)}}\right)^{1/2}\left(\frac{R}{\mathcal{E}_o}\right)^{1/2}\right]$$

Since $\mathcal{E}(z_o)$ has been evaluated from the slope, the intercept is a function of the surface area, distance at the minimum and the potential. No one of these quantities can be determined from the intercept alone. The potential can, however, be found from the deviation of the data from a straight line. The data can be either fit to Equation 10 or 34 to find the values of m and n in Equation 35. This can only be achieved for accurate data obtained in the range of $t < 5$. The best region is t approximately one. Thus far this has not been achieved, except possibly for helium and neon (16).

In any event there is no way within the framework of the theory to separate A and z_o, and hence one must resort to

methods external to the theory. Thus far, two methods have been advanced for the evaluation of z_o and hence, indirectly, the area.

The first method determines the value of z_o as the arithmetic mean of the radii of the adsorbent and adsorbate. In order to find the radius of the adsorbate, a knowledge of its physical state is necessary. In the case of non-spherical molecules, the orientation with respect to the surface must also be known. These things are not known at the present time; therefore, the areas obtained in this way are of semi-quantitative significance.

The second method involves knowing the dependence of z_o on $\mathcal{E}(z_o)$. The best attempt in this regard was by Kirkwood (8) and Müller (9), but this also is only of semi-quantitative significance. It should be noted however, that the areas obtained in this way agree well with the first method when crystal radii are employed (16).

All of these arguments apply to an equilibrium system. Despite the fact that chromatography data is obtained with a dynamic system, it can be shown that it is also an equilibrium system in the following way.

Workers in the field of gas chromatography have observed that the retention volume, defined as the product of the retention time and the volume flow rate, is a constant with respect to flow rate over a wide range of flow rates. (The

retention time is the time it takes for a gas to pass through the packed column.) This implies that the gas is in equilibrium with the solid. Another way of saying this is that the rates of adsorption and desorption are fast compared with the flow rate. With this apparently justifiable assumption, chromatographic data can be related to data obtained with a static system.

The retention volume of a gas G is just the apparent volume of the gas. If the gas is ideal, then the retention volume is the geometric volume of the system. The difference between these two quantities is simply $-\beta A$. However, it should be noted that one never passes just one gas through the column; it is always a mixture of the gas G and the carrier gas. In this case the carrier gas must be ideal if the difference in the volumes measured is equated to $-\beta A$.

One estimate of the ideality of a gas is its second virial coefficient. The second virial coefficients of helium, neon and hydrogen are small in comparison with gases such as nitrogen or the hydrocarbons. A second measure of the ideality of neon under the conditions of the experiment is its change in retention volume with temperature. It was found that neon obeyed the ideal gas law within experimental error over the temperature range, $300^{\circ}K$ to $700^{\circ}K$. Hence, to a good approximation, the difference between the retention volumes of gas G and neon with helium as the carrier gas is a measure of $-\beta A$.

The retention time is measured under column conditions while the flow rate is measured at room temperature and pressure. In order to obtain the retention volume under column conditions, it is necessary to correct the flow rate to column conditions. Since the quantity of gas introduced is small, approximately 0.1 cc., it may be considered to be an ideal gas. In this case the retention volume V_R is corrected according to

$$V_R = Ft_R(T_c/T_o)(P_o/P_c)$$

where the subscripts c and o refer to column and output respectively. F is the flow rate: t_R is the retention time; T is the absolute temperature and P is the pressure.

Since a pressure gradient exists across the column, the meaning of P_c is not immediately obvious. It can be determined, however, if viscous flow through a capillary is assumed to represent the flow through the column. In this case the pressure at a point z along a column of length L is given by

$$P_z^2 = P_o^2 + \frac{P_i^2 - P_o^2}{L} z$$

where P_i and P_o are the inlet and outlet pressures respectively. The ratio of pressures can then be shown to be given by

$$\frac{P_o}{P_c} = \frac{2}{3} P_o \quad \frac{P_i^2 - P_o^2}{P_i^3 - P_o^3} = \frac{P_o}{P_m} \left\{ 1 - \frac{1}{12} \left(\frac{\Delta P}{P_m} \right)^2 \right\}$$

where P_m is the arithmetic mean pressure and ΔP is the pressure gradient across the column. The retention volume corrected to column conditions is given by

$$V_R = F t_R \frac{T_c}{T_o} \frac{P_o}{P_m} \left\{ 1 - \frac{1}{12} \left(\frac{\Delta P}{P_m} \right)^2 \right\}$$

RESULTS AND DISCUSSION

The interaction of the gases argon, nitrogen, carbon monoxide, methane, ethane, ethylene, propane and propylene was studied with a "Columbia L" activated charcoal surface by Gas Adsorption Chromatography. The particle size was 20 to 40 mesh. The raw chromatographic data was processed on a computer (Appendix C) to give $-\beta A$ ($= \lim_{p \to 0} \left[\frac{NkT}{p} - V\right]$ as a function of temperature. The results are shown graphically in Figures 5, 6, and 7. According to the empirical relation given by Hansen (13), ln $(-\beta A)$ should be a linear function of $1/T$ and indeed, this is the case.

Since the accuracy of the experimental data did not permit unambiguous evaluation of the potential, the gases studied were assumed to obey the 9-3 potential. The data was analyzed in two ways. The first method consisted of finding the best straight line through the experimental points when ln $(-\beta A T^{-1/2})$ is plotted versus $1/T$. This treatment assumes that Equation 34 with S_n approximately one and $R(t)$ small represents the data. The slope is $\varepsilon(z_o)/R$ and the intercept is related to ln Az_o. The results of this analysis are presented in Table 2.

The second method involved fitting the experimental data to the exact theoretical curve, Equation 17. A value of $\varepsilon(z_o)/R$ was assumed and ln Az_o calculated. $\varepsilon(z_o)/R$ was then systematically varied until the sums of the squares of the

Figure 5. Chromatographic Data Run No. 1

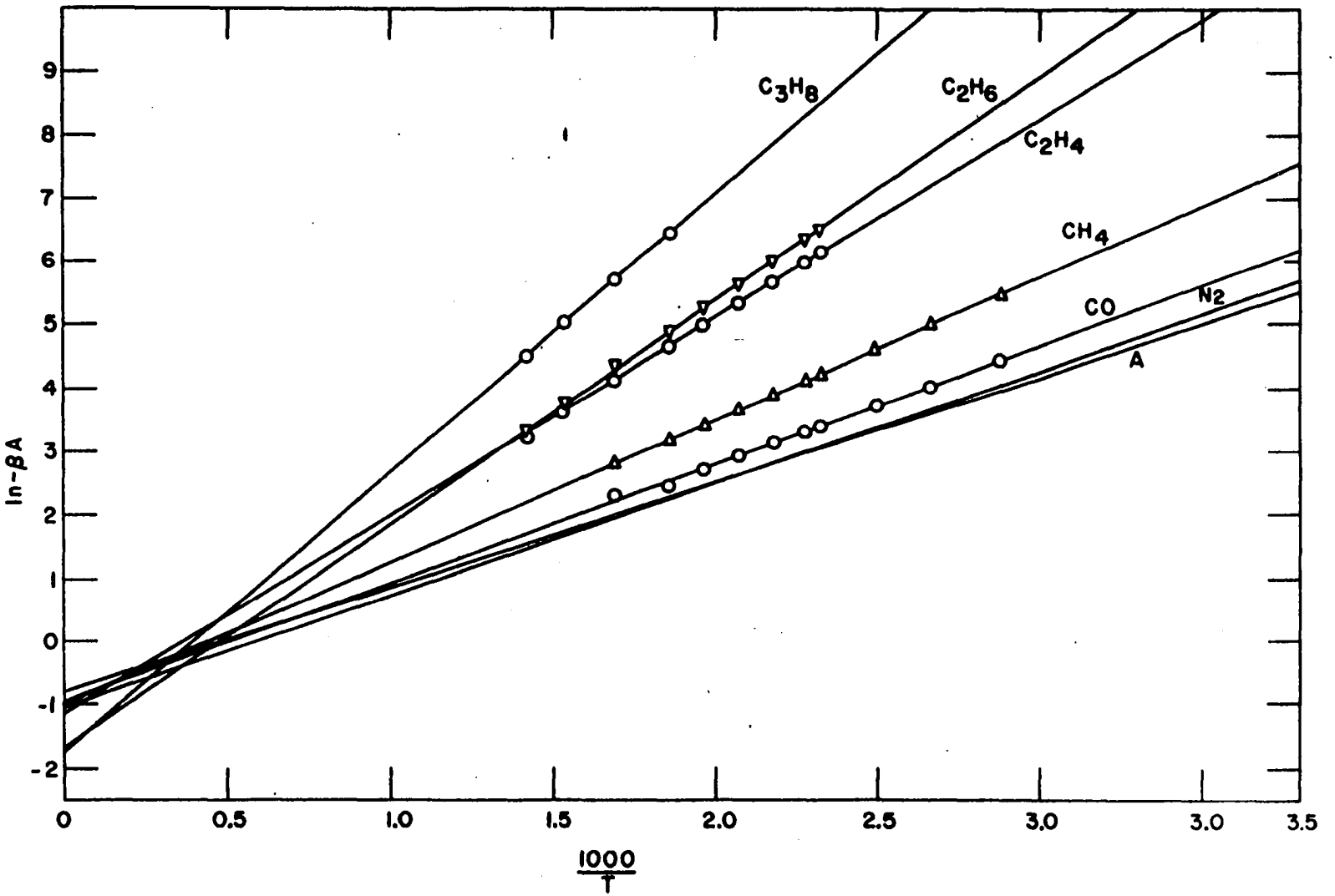
C_3H_8
C_2H_6
C_2H_4
CH_4
CO
N_2
A
$\ln -\beta A$
9
8
7
6
5
4
3
2
1
0
-1
-2
0
0.5
1.0
1.5
2.0
2.5
3.0
3.0
3.5
$\frac{1000}{T}$

Figure 6. Chromatographic Data Run No. 2

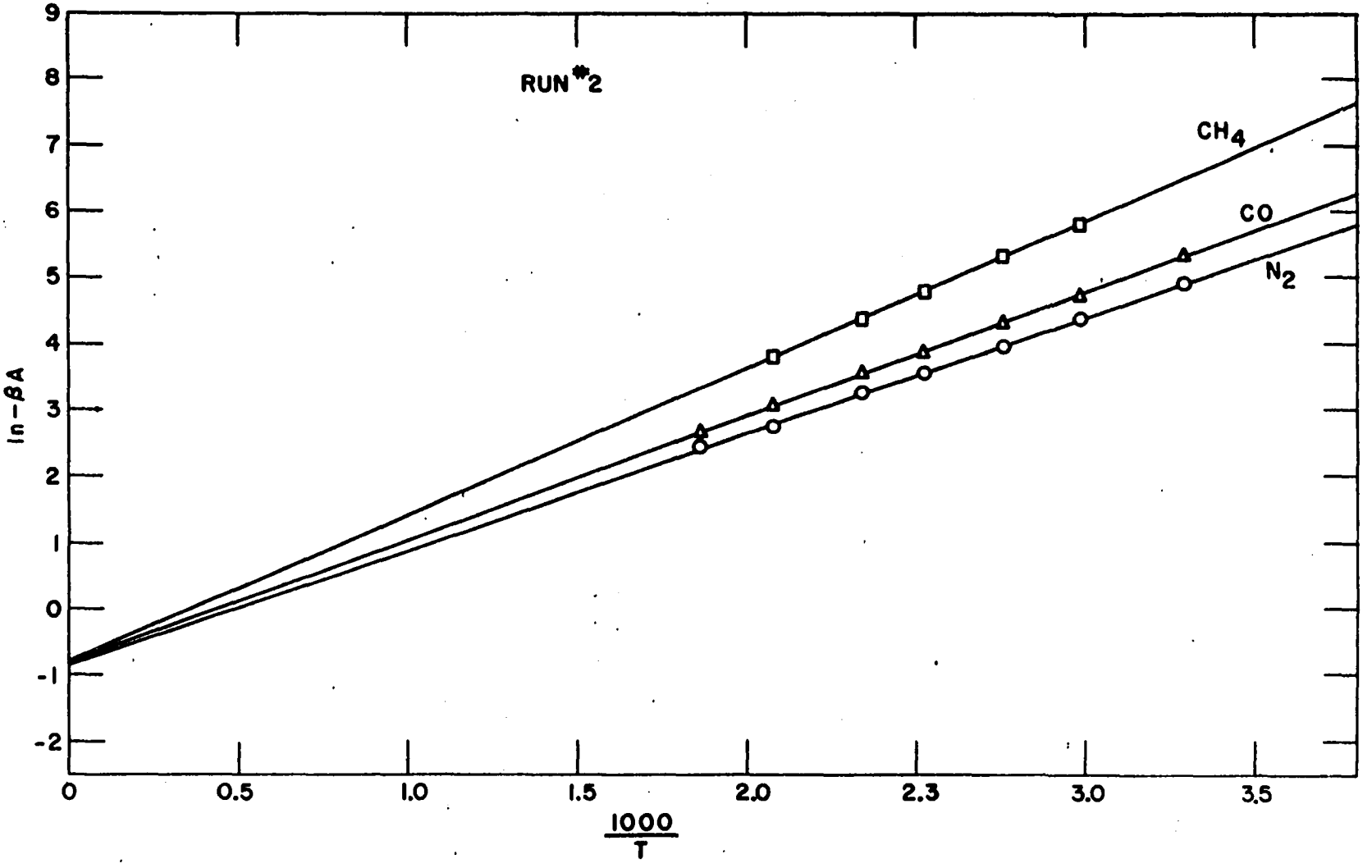
RUN #2
CH4
CO
N2
ln −βA
9
8
7
6
5
4
3
2
1
0
-1
-2
0
0.5
1.0
1.5
2.0
2.3
3.0
3.5
1000/T

Figure 7. Chromatographic Data Run No. 3

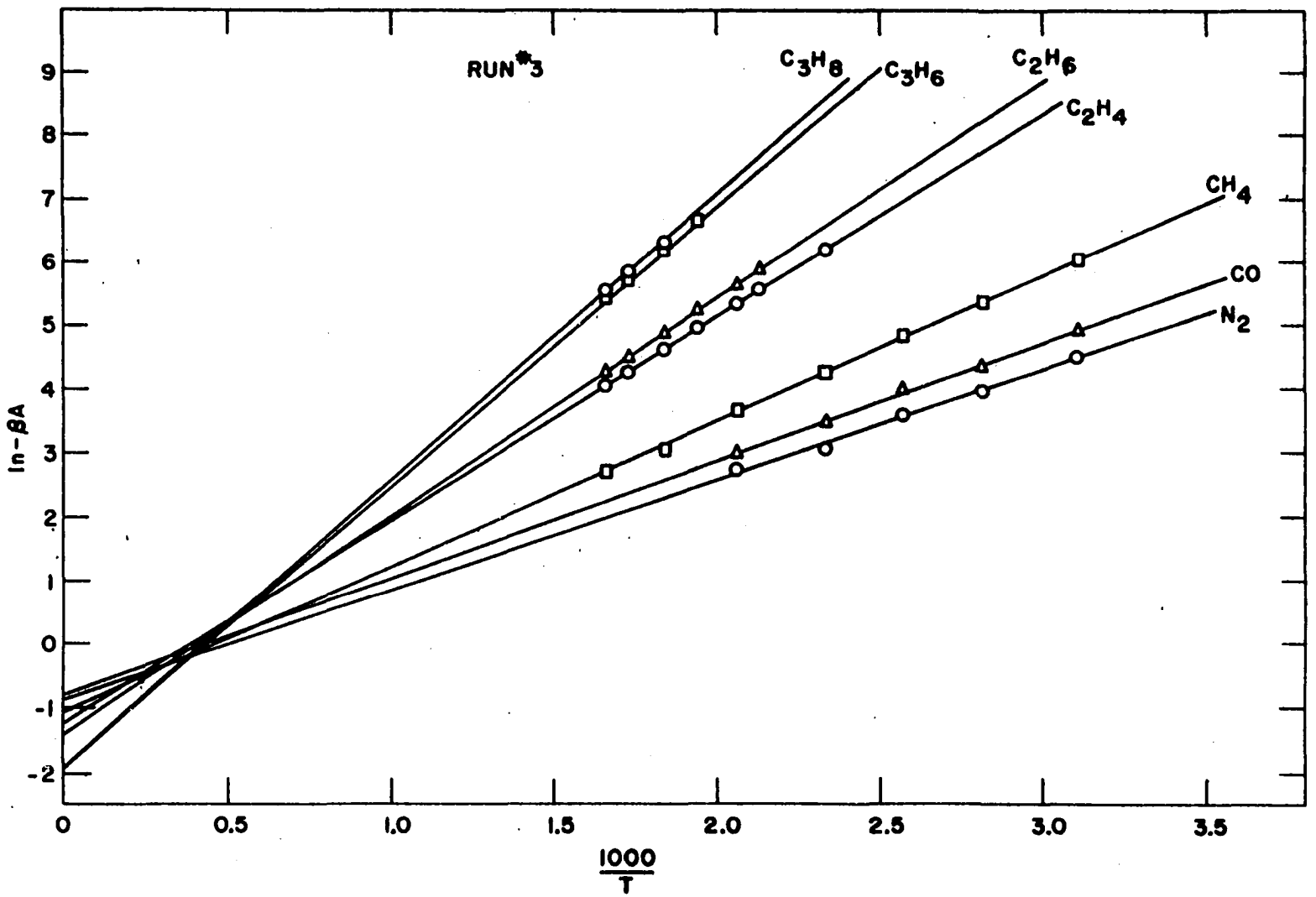
RUN #3
C_3H_8
C_3H_6
C_2H_6
C_2H_4
CH_4
CO
N_2
ln-βA
9
8
7
6
5
4
3
2
1
0
-1
-2
0
0.5
1.0
1.5
2.0
2.5
3.0
3.5
1000/T

Table 2. Parameters evaluated from the limiting form of Equation 34

Gas	ε_o/R	$-\ln(Az_o)$	Standard deviation
A	1882	1.82	0.04
N_2	2018	2.07	0.04
CO	2089	1.92	0.04
CH_4	2463	1.86	0.03
C_2H_4	3467	2.10	0.01
C_2H_6	3667	2.16	0.02
C_3H_8	4715	2.85	0.006
A	1885	1.77	0.02
N_2	1950	1.85	0.03
CO	2062	1.79	0.02
CH_4	2414	1.69	0.007
A	1794	1.58	0.05
N_2	1926	1.85	0.05
CO	2039	1.74	0.03
CH_4	2510	1.95	0.02
C_2H_4	3448	2.05	0.01
C_2H_6	3689	2.21	0.01
C_3H_6	4709	2.62	0.01
C_3H_8	4781	2.61	0.01

deviations of the points from the curve was a minimum. This operation was carried out on a computer (Appendix C) and the results are given in Table 3.

The values of $\mathcal{E}(z_o)/R$ presented in the tables are in agreement with those of Hanlan and Freeman (18) on the same type of charcoal. The agreement was within three percent in all cases where comparisons could be made. Their values for $\ln Az_o$ were smaller than those reported here. Since the particle size of the charcoal used in their experiments was larger (8 to 14 mesh), it is not unlikely that this result is due to their charcoal having a smaller surface area. The trend in $\ln Az_o$ was the same as that reported in Tables 1 and 2.

The values of $\mathcal{E}(z_o)/R$ contained in Tables 2 and 3 agree within experimental error. The observed trend in $\mathcal{E}(z_o)$ is to be expected since it is the same trend that exists for gas-gas interactions except for argon. $-\mathcal{E}(r_o)$ for the Lennard-Jones 12-6 potential for argon is greater than the corresponding values for nitrogen and carbon monoxide, while $-\mathcal{E}(z_o)$ for argon is less than either of these two gases. This exception can be attributed to orientation effects.

The polarizability of a non-spherical molecule is anisotropic. In the cases of nitrogen and carbon monoxide, the polarizability is greater parallel to the bond than perpendicular to it. Since the polarizability is proportional to $\mathcal{E}(z_o)$, $\mathcal{E}(z_o)$ will depend on the orientation of the molecule

Table 3. Parameters evaluated from Equation 17.

Gas	ε_o/R	$-\ln(Az_o)$	Standard deviation
A	1896	2.06	0.05
N_2	2056	2.36	0.05
CO	2135	2.22	0.07
CH_4	2525	2.18	0.03
C_2H_4	3562	2.43	0.01
C_2H_6	3752	2.46	0.02
C_3H_8	4816	2.77	0.01
A	1923	2.06	0.03
N_2	1998	2.16	0.02
CO	2110	2.09	0.01
CH_4	2487	2.02	0.01
A	1821	1.86	0.04
N_2	1976	2.17	0.05
CO	2088	2.05	0.03
CH_4	2578	2.16	0.02
C_2H_4	3538	2.38	0.01
C_2H_6	3778	2.51	0.01
C_3H_6	4790	2.87	0.01
C_3H_8	4868	2.87	0.01

with respect to the surface. Since the magnitude of gas-gas interactions is much smaller than gas-solid interactions, $\epsilon(r_o)$ will not reflect orientation effects to as great an extent. Hence, it is not unreasonable to expect the interaction of nitrogen and carbon monoxide with the surface to be stronger than that of argon.

The agreement between the two methods is much less satisfactory for the parameter ln Az_o. This parameter, as can be seen from Equation 36, is very sensitive to the slope and the deviation of the curve from linearity. Since much of the data was obtained in the region where the terms in $1/t$ and $1/t^2$ were not small, the assumption that S_n is approximately one is not satisfactory. It is for this reason that the values of the parameter lnAz_o are not in agreement and that Table 3 contains the more accurate values. Therefore, the discussion will be limited to the parameters contained in Table 3.

The first observation one makes is that the values of ln Az_o for the same gas, but from different runs, do not agree within the standard deviation listed. The standard deviation, however, reflects the error in the fit and not necessarily the error in ln Az_o. As a matter of fact, an analysis of the evaluation of ln Az_o reveals that the standard deviation is not a measure of the accuracy of ln Az_o.

If it is assumed that ln $(-\beta AT^{-1/2})$ or ln $(-\beta A)$ is a

linear function of 1/T, then the effect of an error in $\varepsilon(z_o)/R$ on the intercept can be found. This will give an idea as to the accuracy with which the intercept can be found from experimental data. Any error in the intercept will contribute to the uncertainty of ln Az_o.

For example, if one considers the temperature range over which data were obtained for the gases nitrogen, argon, carbon monoxide and methane, it is found that an uncertainty of 25° in $\varepsilon(z_o)/R$ will result in an uncertainty of 0.06 in the intercept. Similar results are found for the other gases. In the case of methane, this means that an error of one percent in $\varepsilon(z_o)/R$ results in a six percent error in Az_o. If one accepts the reproducibility of $\varepsilon(z_o)/R$ as a measure of its uncertainty, then the values cited above are underestimates of the uncertainty in the intercept. These results reflect the accuracy with which ln Az_o can be determined by gas chromatography.

A similar result is observed if one investigates the process by which the experimental data is fit to Equation 17. However, a separate analysis must be made for each gas. For example, if one considers the data for nitrogen, carbon monoxide and methane in the first run, the standard deviations of the data from theoretical curves are found to remain essentially unchanged as the parameters $\varepsilon(z_o)/R$ and ln Az_o are varied over the following ranges: for nitrogen, 2080≥

$(z_o)/R \geq 2000$ and $-2.25 \geq \ln Az_o \geq -2.41$; for carbon monoxide, $2120 \leq \epsilon(z_o)/R \leq 2160$ and $-2.20 \geq \ln Az_o \geq -2.26$; for methane, $2520 \leq \epsilon(z_o)/R \leq 2540$ and $-2.08 \geq \ln Az_o \geq -2.20$.

Hence, quite apart from the theoretical ambiguities involved in the determination of the surface area from the intercept, there is also an experimental uncertainty of the order of six to ten percent which arises from the mechanics of curve fitting despite the fact that the raw data appear to be accurate within two percent.

The evaluation of z_o has been discussed previously (page 35) and will not be repeated here. In the following discussion, z_o will be assumed to be the sum of the van der Waals radii of the adsorbent and the adsorbate. The van der Waals radius of the adsorbent will be assumed to be one half of the interplanar spacing in graphite, while the van der Waals radius of the adsorbate is obtained from second virial coefficient data.

It may be first be noted from Table 3 that $\ln Az_o$ is a constant for nitrogen, carbon monoxide and methane. Since the van der Waals radii of these gases are approximately constant at 1.88 $\mathring{A}$, the area calculated will be 330 m^2/gm. For the remaining gases used in these experiments, the area decreases with increasing size of the adsorbate molecule. This trend seems to appear in all methods for determining the surface area from adsorption data. The usual explanation is

that the surface is not smooth, but consists of a series of cracks, crevices and pores of varying size. A portion of the surface is inaccessible to the larger molecules and hence the calculated area should decrease with increasing size of the adsorbate molecule. This explanation is plausible for the substrate used in these experiments since it is known to be porous. Rough calculations indicate that the gas spends sufficient time to diffuse into pores even if they run the entire length of the carbon particle. There are, however, a number of adsorbents that are believed to be smooth, yet the trend persists.

In a series of experiments of the adsorption of the rare gases with a highly graphitized carbon black by Halsey and coworkers (16), the surface area calculated depended on the adsorbate molecule regardless of the method used to evaluate z_o. The most anomalous feature of their results was that, although the general trend of decreasing area with increasing size of the adsorbate molecule was present, krypton gave a lower area than either argon or xenon. This anomaly was present for the 9-3, 12-3 and ∞-3 potential models. These data are considered by Halsey to be among the most accurate data obtained in his group, and represent a trend in the opposite direction to that expected if there were pores, cracks or crevices. Another interesting aspect of their results is that the normal trend of decreasing area with

increasing size of the adsorbate molecule is observed when the same data are analyzed in terms of the 10-4 potential model, but the standard deviation in the fit has increased slightly.

It is apparent that there is some uncertainty in the area measured according to this theory. A six to ten percent error in the area results solely from intercept uncertainty in the curve-fitting process. Another error of about ten percent arises from ambiguity in z_o. This means that even if the force law for gas-solid interactions was the same for all gases, the relative areas would be uncertain to about 20 percent. The next question to arise is the relation of the area calculated to the actual area of the surface.

In order to answer this question, it is necessary to have an independent method for the evaluation of the area. As far as this author is concerned, there is no method that will give the actual area of the surface. The most widely used method, however, is the Brunauer-Emmett-Teller (BET) method for estimating surface area.

The BET method provides a scheme for estimating, from the form of an adsorption isotherm, the number of molecules required to furnish a close-packed monomolecular film on the surface of an adsorbent. The area of the adsorbent is then obtained by multiplying this number by a van der Waals cross sectional area of the adsorbed molecule (estimated, for

example, from the liquid density or from the crystal structure of condensed phases of the adsorbed molecule). The theory behind this scheme, in the case of non-porous adsorbents, has been shown by Halsey (23) to be based on untenable assumptions, and the estimation of monolayer coverage based on it must hence be considered to have at most an empirical justification at present. Nevertheless, this method is the basis for the vast majority of reported surface areas.

In the case of porous adsorbents, isotherms for the adsorption of condensible vapors show generally sharp limiting values as pressure is increased. The BET treatment ascribes this limit to the formation of a complete monolayer, and claims that for such adsorbents further adsorption is prevented sterically. On this basis surface areas as great as 2500 m^2/gm have been reported for some charcoals. Pierce, Wiley, and Smith (24) have pointed out that the apparent areas of such materials decrease markedly when estimated with molecules of increasing size, but that the product of the limiting number of moles adsorbed and the adsorbate (liquid) molar volume is nearly independent of molecular size. They have, therefore, claimed that this method measures the adsorbent pore volume rather than the surface area.

The area of Columbia L charcoal was measured by the BET technique and found to be 1000 m^2/gm. In view of the foregoing comments, it is believed that this value need not be

accepted as an absolute standard for the surface area in any sense.

One must conclude that there is at present no method for obtaining absolute surface areas with which those obtained by means of the present theory can be compared. The method tested in this work appears theoretically sound, and there also appears to be good reason for expecting the potential energy for gas-solid interaction to be very nearly of the form $\varepsilon(x) = - Ax^{-3} + Bx^{-9}$. The principle uncertainties involved in area estimation are, therefore, a curve fitting error of the order of magnitude of ten percent, and an uncertainty in z_o (distance of the molecule from the surface at the potential minimum) which is at least of similar magnitude. The latter error would be similar in character for a set of similar adsorbents, so that area ratios obtained by this method would be more reliable than the individual areas.

SUMMARY

The determination of the surface area of an adsorbent has been one of the foremost problems in surface chemistry. The BET method has been and still is the method most commonly used for the estimation of surface areas despite the fact that it is theoretically untenable.

Halsey and coworkers introduced a method for the determination of surface areas based on a model quite analogous to the theory of the second virial coefficient. If $\lim_{p\to 0}\left[\frac{NkT}{p} - V\right]$ is measured as a function of temperature, it is theoretically possible to determine the energy of adsorption, the surface area and the force law for the gas-solid interaction.

Since the retention volume in gas chromatography is a constant with respect to flow rate, the implication is that the gas is in equilibrium with the solid surface and hence, chromatographic data can be interpreted in terms of this theory. Gas chromatography being much more versatile than conventional adsorption techniques, seems to be an attractive method for these measurements. Although at the present time it is less accurate than static measurements, the ease with which data can be obtained and the wide temperature range available for experiments make it a useful tool for the surface chemist.

The chromatographic data obtained by this author was

interpreted in terms of this model. The energy of adsorption was found for a number of gases adsorbed on "Columbia L" activated charcoal. The surface area, although 20 to 30 percent uncertain, was also found. The uncertainty in the area obtained led us to investigate the original theory of Halsey and coworkers. For this purpose an asymptotic expansion valid for low temperatures was developed. This enabled us to reinterpret the evaluation of the parameters and establish the limits with which the surface area could be obtained from chromatographic data. A less thorough analysis of the data considered by Halsey and coworkers to be their most accurate made it possible to establish the reliability of the surface areas determined from static measurements.

The asymptotic expansion has been shown to be valid for $\varepsilon(z_o)/RT$ ($\varepsilon(z_o)$ is the depth of the potential well.) greater than five. Since it is much simpler to use, it should find wide spread applicability.

BIBLIOGRAPHY

1. Eucken, A. Verhandlungen der Deutschen Physikalischen Gesellshaft. 16: 345. 1914.

2. Eucken, A. Zeitshrift für Electrochemie. 28: 6. 1922.

3. Polanyi, M. Verhandlungen der Deutschen Physikalischen Gesellshaft. 18: 55. 1916.

4. London, F. Zeitshrift für physikalische Chemie (Leipzig), Series B, 11: 222. 1930.

5. Margenau, H. Reviews of Modern Physics. 11: 1. 1939.

6. Orr, W. J. C. Transactions of the Faraday Society. 35: 1247. 1939.

7. Kiselev, A. Transactions of the Faraday Society. 59: 176. 1963.

8. Kirkwood, J. G. Physikalische Zeitschrift. 33: 57. 1932.

9. Müller, A. Proceedings of the Royal Society (London), Series A, 154: 624. 1936.

10. Steele, W. A. and Halsey, G. D., Jr. Journal of Chemical Physics. 22: 979. 1954.

11. De Marcus, W. C., Hopper, E. H., and Allen, A. M. U. S. Atomic Energy Commission Report K-1222. (Carbide and Carbon Chemicals Corp. K-25 Plant, Oak Ridge, Tenn.) 1955.

12. Freeman, M. P. Journal of Physical Chemistry. 62: 723. 1958.

13. Hansen, R. S. Journal of Physical Chemistry. 63: 743. 1959.

14. Hirschfelder, J. O., Curtiss, C. F., and Bird, R. B. Molecular theory of gases and liquids. New York, N. Y., John Wiley and Sons, Inc. c1954.

15. Constabaris, G., Singleton, J. H., and Halsey, G. D., Jr. Journal of Physical Chemistry. 63: 1350. 1959.

16. Sams, J. R., Jr., Constabaris, G., and Halsey, G. D., Jr. Journal of Physical Chemistry. 64: 1689. 1960.

17. Sams, J. R., Jr. Journal of Chemical Physics. 36: 1334. 1962.

18. Hanlan, J. F. and Freeman, M. P. Canadian Journal of Chemistry. 37: 1575. 1959.

19. Jackson, D. M., Wells, G., and Soseman, D. Unpublished multilithed paper. U. S. Atomic Energy Commission. Ames Laboratory. Contribution No. 957. 1960.

20. Fowler, R. H. and Guggenheim, E. A. Statistical thermodynamics. New York, N. Y., Cambridge University Press. 1960.

21. Schmauch, L. J. and Dinerstein. R. A. Analytical Chemistry. 32: 343. 1960.

22. Madison, J. J. Analytical Chemistry. 30: 1859. 1958.

23. Halsey, G. Journal of Chemical Physics. 16: 931. 1948.

24. Pierce, C., Wiley, J. W. and Smith, R. N. Journal of Physical Chemistry. 53: 669. 1949.

ACKNOWLEDGEMENTS

I wish to express my deep appreciation to Dr. Hansen for suggesting this problem and for the help and encouragement he gave while this work was performed. His deep insight into the theoretical aspects of this problem was invaluable. His suggestions and help made the completion of this work possible.

I also wish to express my thanks to Cathy for making the last two years here, the best two.

Lastly, credit should be given to Tom McGee for writing and debugging the curve fitting program. The help he gave me with the other programs is also appreciated.

APPENDIX A: THERMAL CONDUCTIVITY OF HYDROGEN-HELIUM MIXTURES

In the process of obtaining chromatograms of hydrogen with helium as the carrier gas, complex peaks were sometimes observed. When small samples of hydrogen were used, the typical chromatogram was observed (Figure 2). As the sample size was increased, a twin peak was observed. The minimum became deeper with increasing sample size. If the concentration of hydrogen was very high, then the minimum was so large that the two maxima appeared insignificant. However, careful scrutiny revealed the existence of the two maxima.

This phenomenon has been reported previously and attributed to a minimum in the thermal conductivity of the mixture (21,22). This would explain the observed results, but no proof was offered for the existence of a minimum. Since there were no accurate data for the thermal conductivity of these mixtures, we calculated the curve according to Equations 8.2-35, 8.2-36 and 8.2-40 given by Hirschfelder, Curtiss and Bird (14). The resulting curve is given in Figure 8.

It is clear that a shallow minimum exists in the region of 12 mole percent hydrogen. Therefore, the twin peaks observed have a simple explanation. Since the response of the katharometer detector is proportional to the difference in thermal conductivities between helium and the mixture, concentrations of hydrogen less than 12 mole percent will produce the normal chromatogram. However, the peak is in the

opposite direction to that expected if the thermal conductivity was a monotone increasing function of the hydrogen concentration. If the maximum concentration is greater than 12 mole percent, then a minimum will appear. If the distritution of hydrogen is symmetric, for example a distribution due to diffusion, then the minimum will appear at the center of the curve. But even in cases where the distribution is unsymmetrical, the heights of the two maxima will be identical. If the concentration of hydrogen is large, then the depth of the minimum will be so great that the two maxima will appear insignificant.

Hence, the calculated dependence of the thermal conductivity on concentration for this mixture explains the phenomenon. The exact position of the minimum has not been experimentally verified, but chromatographic results indicate that it would be in the region calculated.

Figure 8. Thermal conductivity of hydrogen-helium mixtures

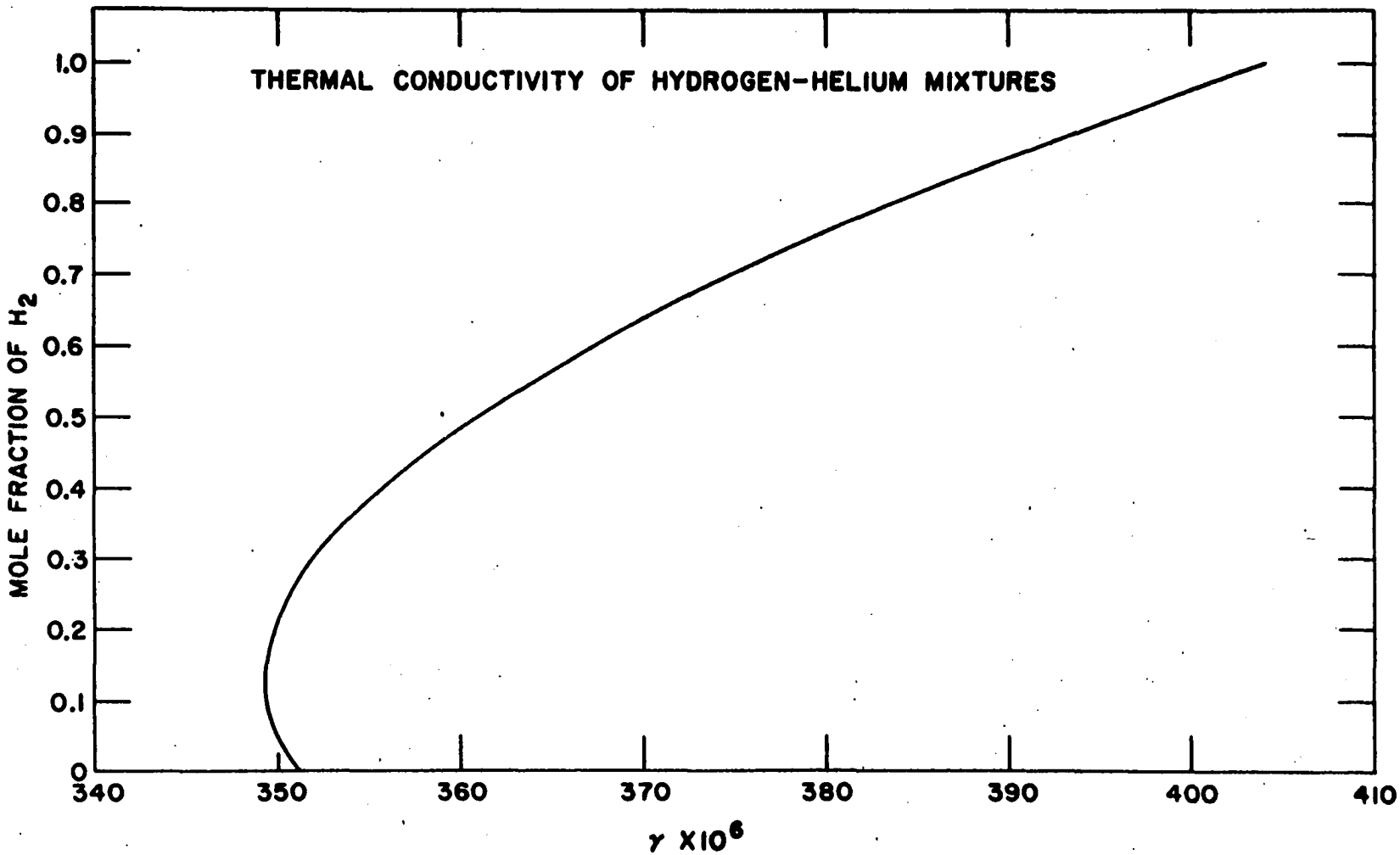
THERMAL CONDUCTIVITY OF HYDROGEN-HELIUM MIXTURES
MOLE FRACTION OF H_2
1.0
0.9
0.8
0.7
0.6
0.5
0.4
0.3
0.2
0.1
0
340
350
360
370
380
390
400
410
$\gamma \times 10^6$

Figure 9. ∞-3 potential model

Program nomenclature

u is t

S_n is $-\beta A/Az_o$

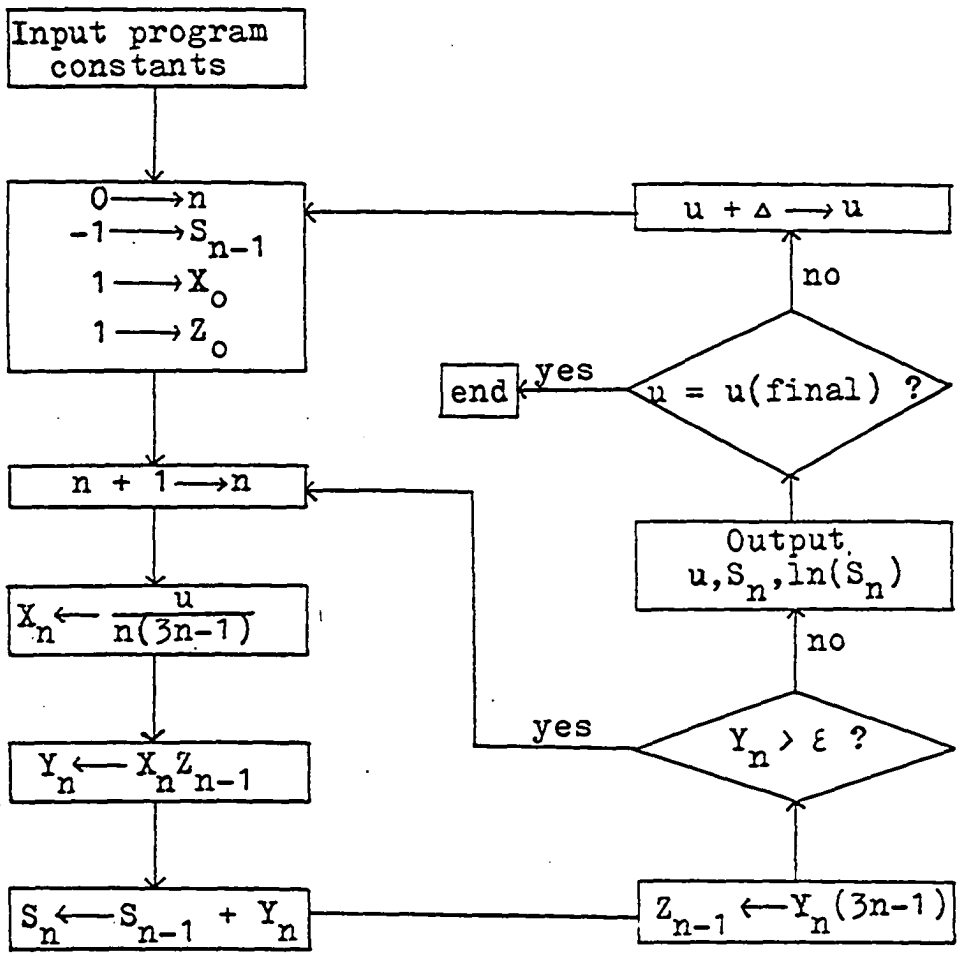
Input program constants
0 → n
-1 → S_{n-1}
1 → X_o
1 → Z_o
n + 1 → n
$X_n \leftarrow \frac{u}{n(3n-1)}$
$Y_n \leftarrow X_n Z_{n-1}$
$S_n \leftarrow S_{n-1} + Y_n$
$Z_{n-1} \leftarrow Y_n(3n-1)$
$Y_n > \varepsilon$?
yes
no
Output $u, S_n, \ln(S_n)$
u = u(final) ?
yes
end
no
u + Δ → u

Figure 10. 9-3 potential model

Program nomenclature

g_i is $\Gamma((3i-1)/9)/i!$

n is the number of values of t

ϵ is the accuracy of the computation

s is $\ln(-\beta A/Az_o)$

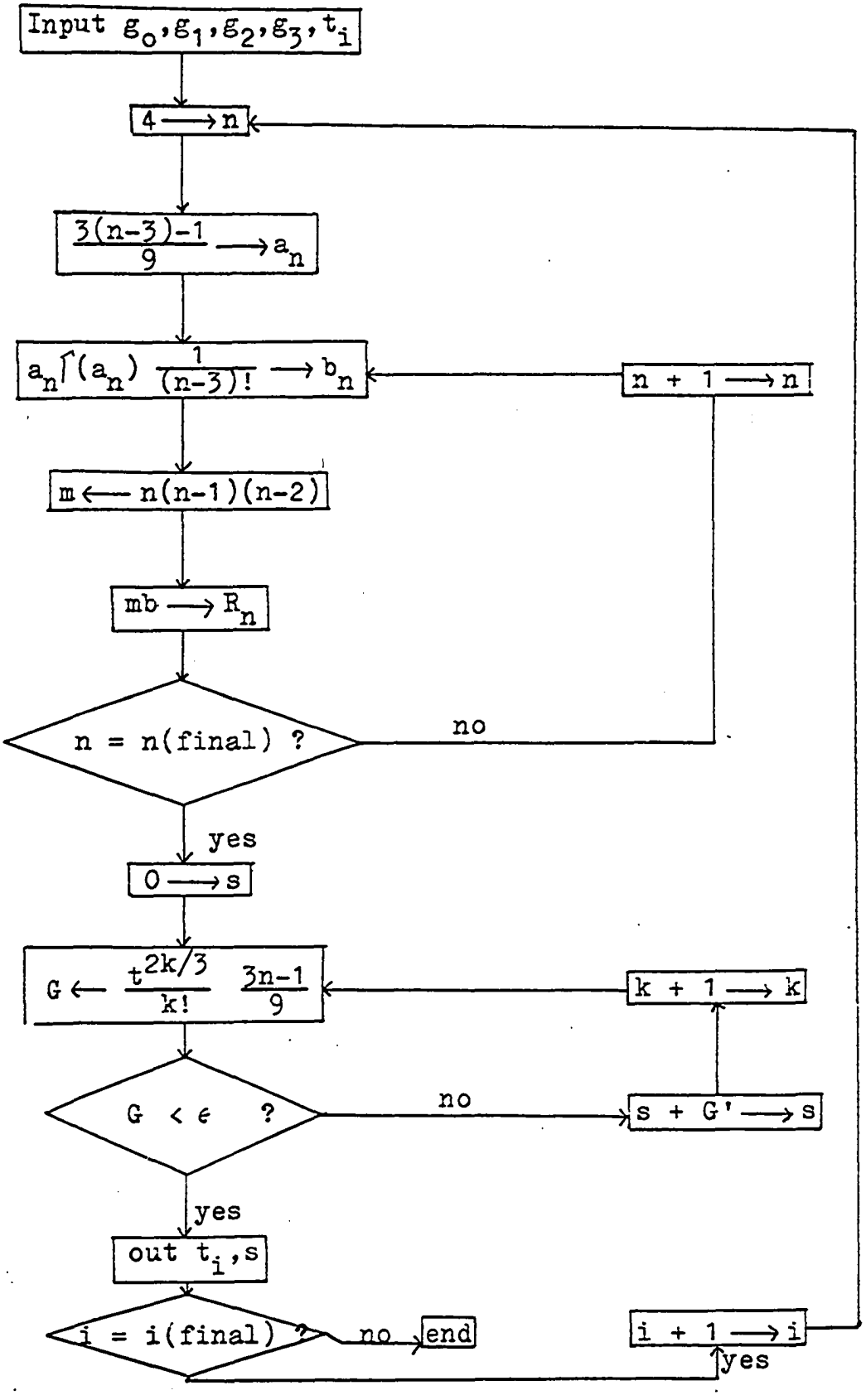
Input g_0, g_1, g_2, g_3, t_i
$4 \longrightarrow n$
$\frac{3(n-3)-1}{9} \longrightarrow a_n$
$a_n \Gamma(a_n) \frac{1}{(n-3)!} \longrightarrow b_n$
$n + 1 \longrightarrow n$
$m \longleftarrow n(n-1)(n-2)$
$mb \longrightarrow R_n$
$n = n(final)$?
no
yes
$0 \longrightarrow s$
$G \longleftarrow \frac{t^{2k/3}}{k!} \frac{3n-1}{9}$
$k + 1 \longrightarrow k$
$G < \epsilon$?
no
$s + G' \longrightarrow s$
yes
out t_i, s
$i = i(final)$?
no
end
$i + 1 \longrightarrow i$
yes

APPENDIX C: PROGRAMS FOR THE EVALUATION OF THE DATA

Figure 11. Program for processing chromatographic data

Program nomenclature

P is barametric pressure

$\overline{\Delta P}$ is the pressure gradient meassured

p is the vapor pressure of water

P_i is the inlet pressure

P_o is the outlet pressure

ΔP is the pressure gradient across the column

P_m is the arithmetic mean pressure

R is the resistance of the platinum thermometer

R_o is the resistance of the platinum thermometer at 0^oC

α and β are constants

V_R is the retention volume

T is the temperature

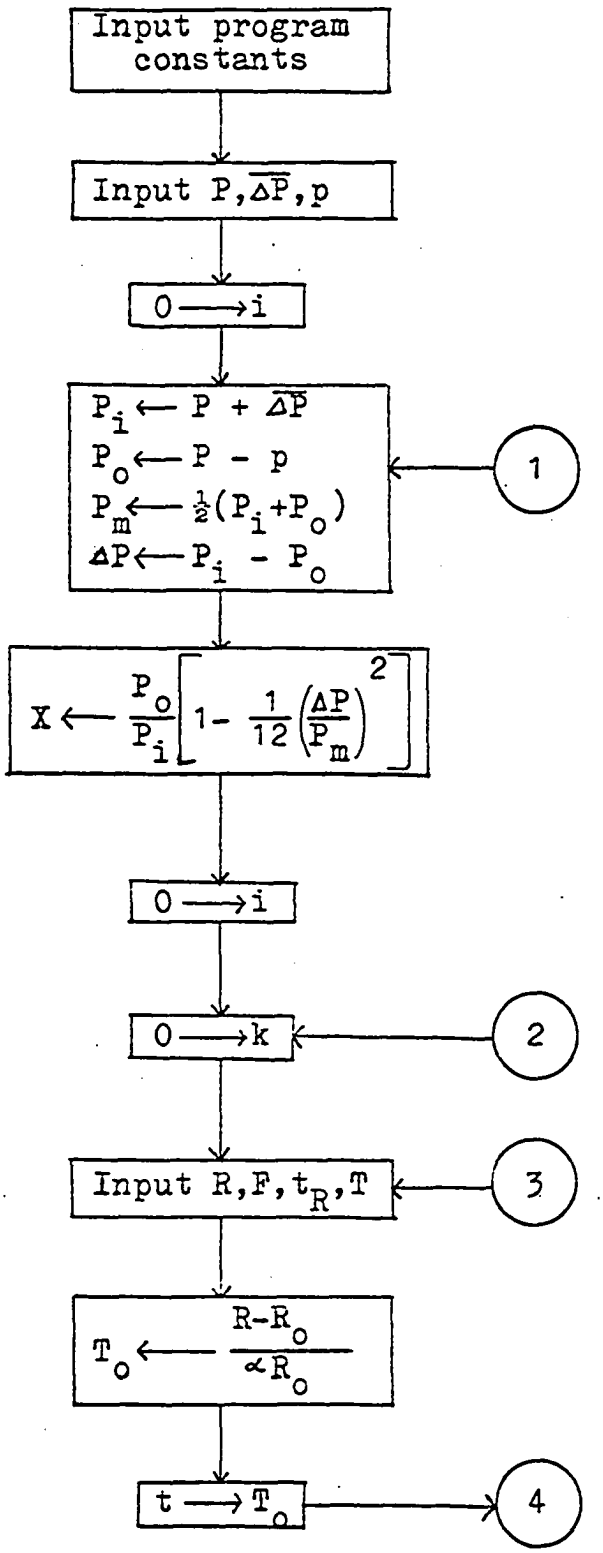
Input program constants
Input P, $\overline{\Delta P}$, p
0 ⟶ i
$P_i \leftarrow P + \overline{\Delta P}$
$P_o \leftarrow P - p$
$P_m \leftarrow \frac{1}{2}(P_i + P_o)$
$\Delta P \leftarrow P_i - P_o$
1
$X \leftarrow \frac{P_o}{P_i}\left[1 - \frac{1}{12}\left(\frac{\Delta P}{P_m}\right)^2\right]$
0 ⟶ i
0 ⟶ k
2
Input R, F, t_R, T
3
$T_o \leftarrow \frac{R - R_o}{\alpha R_o}$
t ⟶ T_o
4

Figure 11. (Continued)

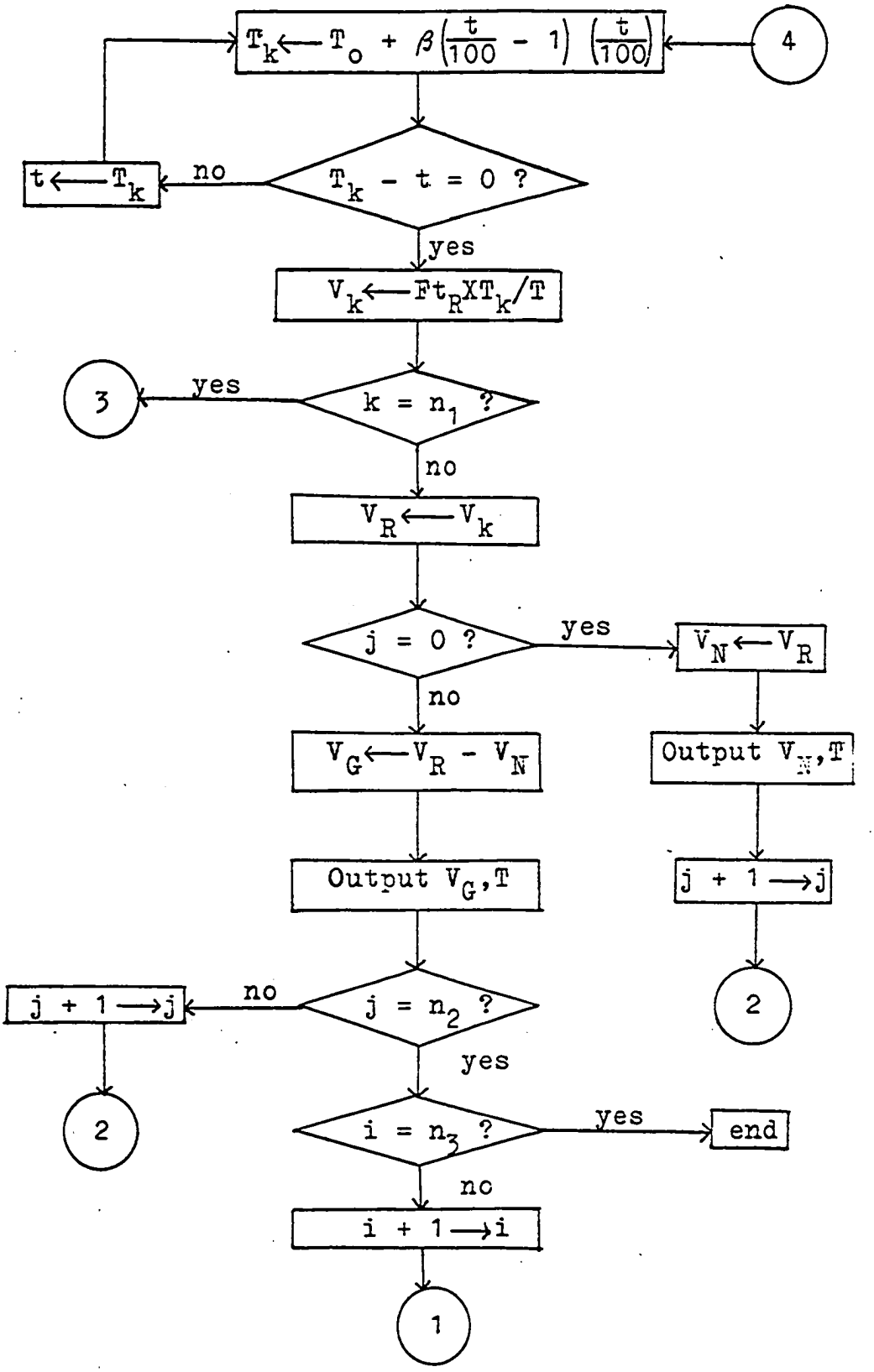
$T_k \leftarrow T_o + \beta\left(\frac{t}{100} - 1\right)\left(\frac{t}{100}\right)$
4
$t \leftarrow T_k$
no
$T_k - t = 0$?
yes
$V_k \leftarrow Ft_R X T_k / T$
3
yes
$k = n_1$?
no
$V_R \leftarrow V_k$
$j = 0$?
yes
$V_N \leftarrow V_R$
no
$V_G \leftarrow V_R - V_N$
Output V_N,T
Output V_G,T
$j + 1 \rightarrow j$
2
$j + 1 \rightarrow j$
no
$j = n_2$?
yes
2
$i = n_3$?
yes
end
no
$i + 1 \rightarrow i$
1

Figure 12. Program for curve fitting to Equation 17

Table nomenclature

V	is the retention volume
V_{geo}	is the retention volume of neon
S'	is the slope of the theoretical curve
G	is the calculated value of Equation 17 for a given t
ϵ	is the accuracy of $\epsilon(z_o)/R$
A	is ln Az_o
S	is the sum of squares of the deviations from the curve

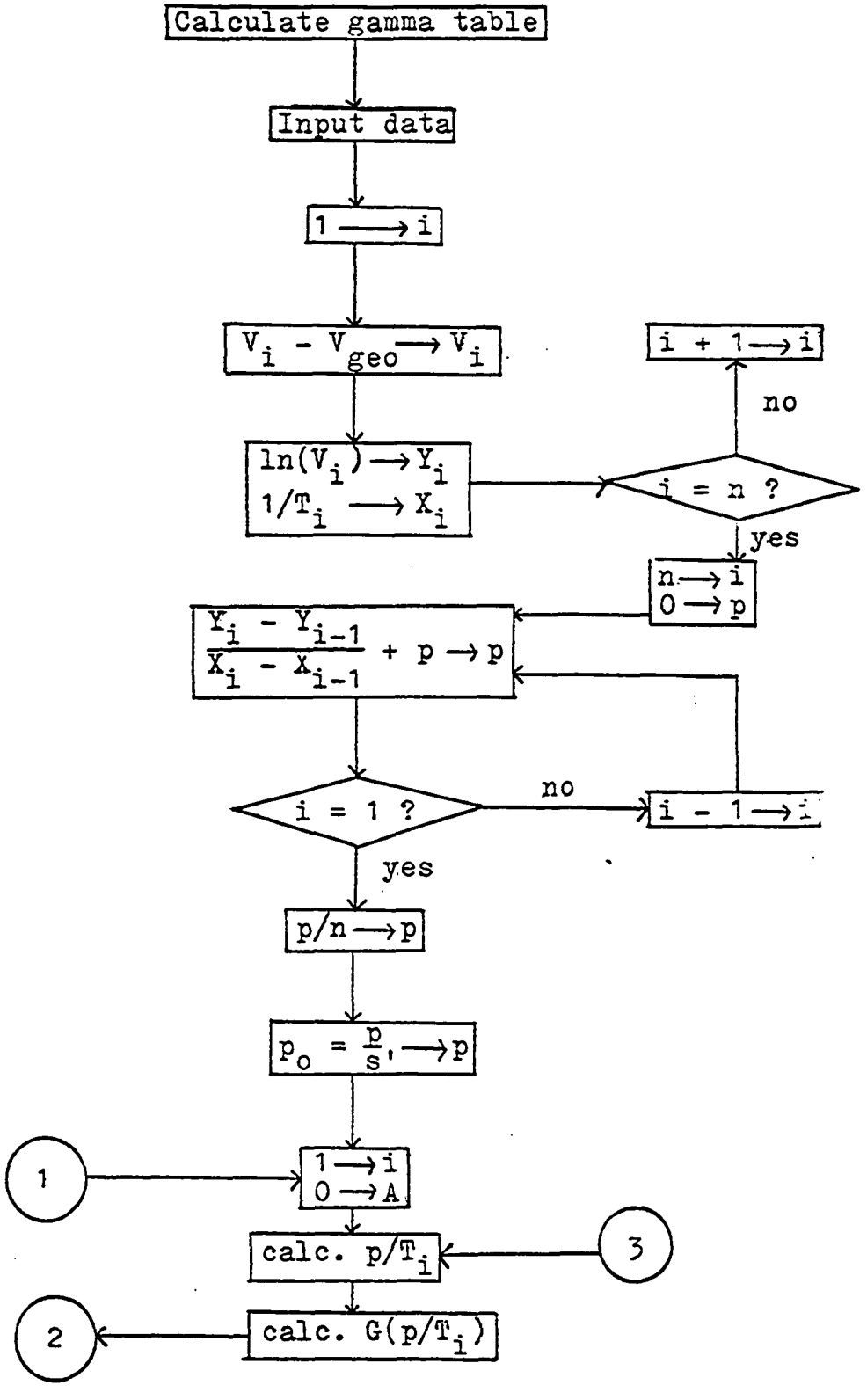
Calculate gamma table
Input data
1 ⟶ i
$V_i - V_{geo} \longrightarrow V_i$
$\ln(V_i) \longrightarrow Y_i$
$1/T_i \longrightarrow X_i$
i = n ?
no
i + 1 ⟶ i
yes
n ⟶ i
0 ⟶ p
$\frac{Y_i - Y_{i-1}}{X_i - X_{i-1}} + p \longrightarrow p$
i = 1 ?
no
i - 1 ⟶ i
yes
p/n ⟶ p
$p_o = \frac{p}{s}, \longrightarrow p$
1
1 ⟶ i
0 ⟶ A
calc. p/T_i
3
2
calc. $G(p/T_i)$

Figure 12. (Continued)

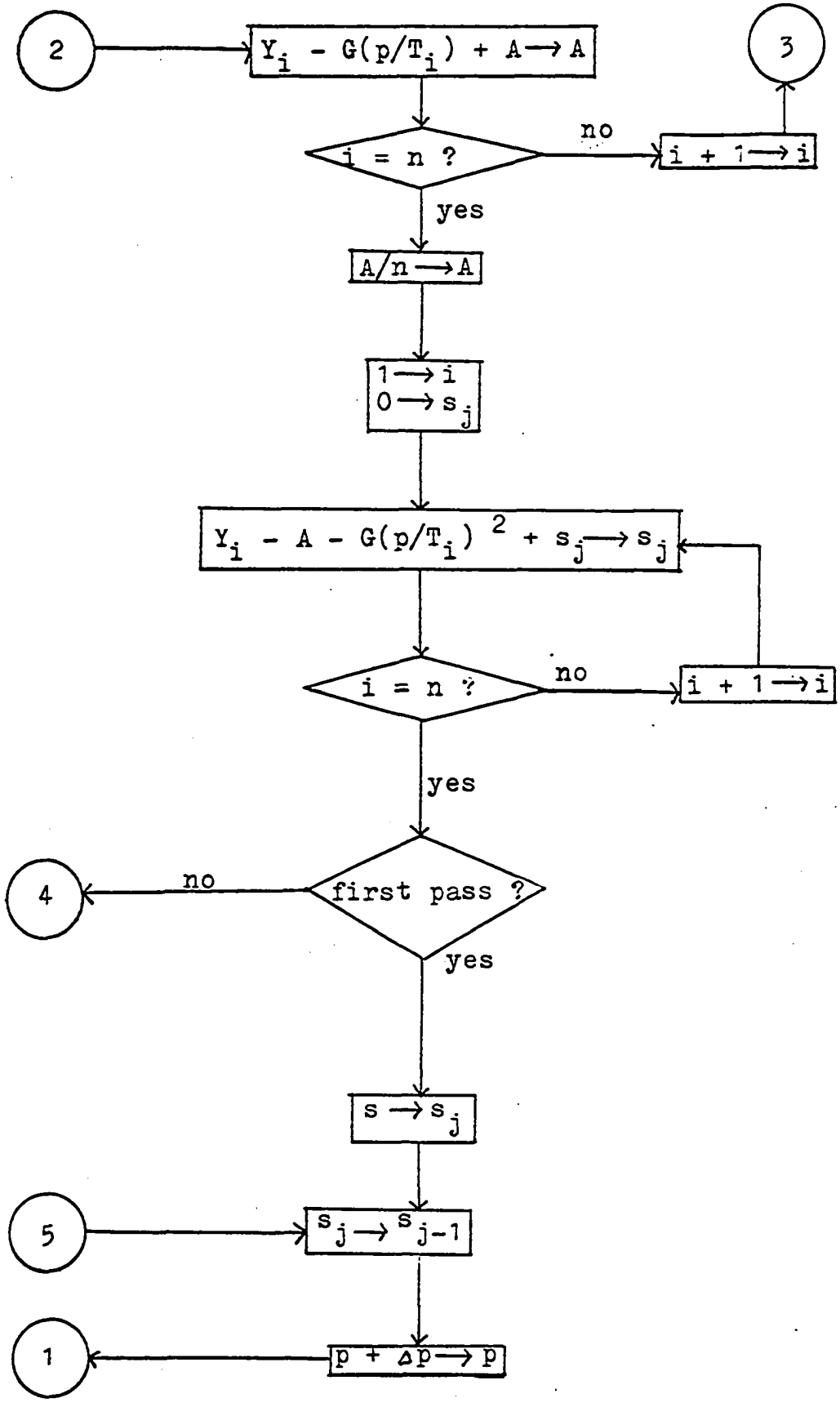
2
$Y_i - G(p/T_i) + A \longrightarrow A$
3
$i = n$?
no
$i + 1 \longrightarrow i$
yes
$A/n \longrightarrow A$
$1 \longrightarrow i$
$0 \longrightarrow s_j$
$Y_i - A - G(p/T_i)^2 + s_j \longrightarrow s_j$
$i = n$?
no
$i + 1 \longrightarrow i$
yes
4
no
first pass ?
yes
$s \longrightarrow s_j$
5
$s_j \longrightarrow s_{j-1}$
1
$p + \Delta p \longrightarrow p$

Figure 12. (Continued)

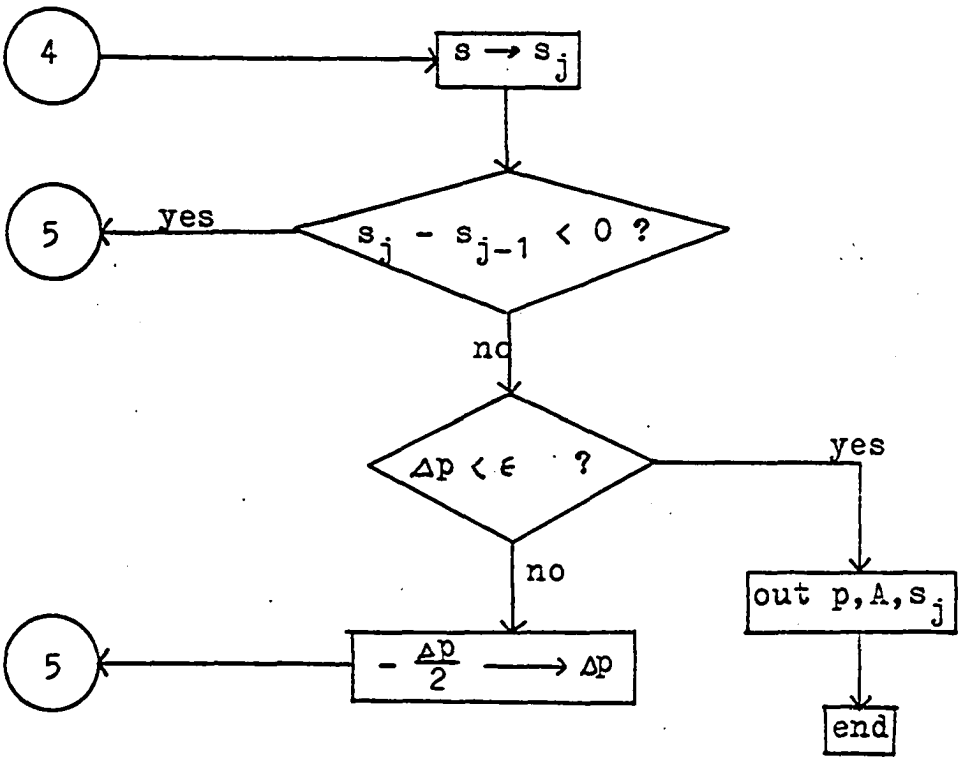
4
s → s_j
5
yes
s_j - s_{j-1} < 0 ?
no
Δp < ε ?
yes
no
out p, A, s_j
5
- Δp/2 → Δp
end

APPENDIX D: SAMPLE CALCULATION OF DATA

The quantities that are obtained in a typical measurement of chromatographic retention time as performed in this thesis are:

1. R_t - the resistance of the platinum thermometer at the temperature of the column in absolute ohms.
2. t_o - the temperature of the flow meter in degrees centigrade.
3. f - the time it takes the film formed from the soap solution to traverse the volume of the flow meter in seconds.
4. d - the distance between the chromatographic peaks in cm.
5. P - barometric pressure in mm of Hg.
6. $\overline{\Delta P}$ - the pressure gradient across the column in mm of Hg.
7. p - the vapor pressure of the soap solution in the flow meter.

From these data it is possible to obtain the volume flow rate, the temperature of both the column and the flow meter, the retention time and the inlet and outlet pressures in the following manner:

$$T_o = t_o + 273.16$$
$$F = (48.712)(60)/f$$
$$t_R = 2d/2.54$$
$$P_i = P + \overline{\Delta P}$$
$$P_o = P - p$$

where all pressures are in mm of Hg, F is in cc/min., t_R is in minutes and T_o is in degrees Kelvin. From these data, the retention volume of the gas V_R is calculated as a function of temperature according to the equation

$$V_R = Ft_R \frac{T_c}{T_o} \frac{P_o}{P_m} \left[1 - \frac{1}{12} \left(\frac{\Delta P}{P_m} \right)^2 \right]$$

The evaluation of this equation was performed on a computer according to the program given in Figure 11. A sample calculation is given below.

For example, a sample set of data is that of neon where

P = 734.77 mm of Hg.
$\overline{\Delta P}$ = 45.0 mm of Hg.
p = 25.76 mm of Hg.
R_t = 32.9742 absolute ohms.
t_o = 26.00 degrees centigrade.
f = 38.25 seconds.
d = 0.481 centimeters.

Hence,

$$V_R = \frac{48.712}{38.25} (60) \frac{(0.481)(2)}{2.54} \frac{346.84}{299.16} (0.95)(1 - 0.0008)$$

$$= 31.8 \text{ cc}$$

Since the pressure gradient across the column is small, between 30 and 60 mm of Hg, the term $\frac{1}{12}(\Delta P/P_m)^2$ is always small, less

than 0.001, and therefore can be neglected with little error.

The data plotted in Figures 5, 6 and 7 were processed in the same manner as the sample calculation given above to give the retention volume as a function of temperature. V_R and V_N represent the retention volumes of the gases and neon respectively. In Table 4, the difference between these two quantities is given as a function of temperature.

Table 4. $-\beta A$ as a function of temperature

Run No.	Gas	V_N(cc)	T(^{o}K)
1	neon	32.00	346.83
		31.63	374.96
		31.39	400.75
		31.42	429.60
		31.50	439.04
		31.20	459.43
		31.24	482.63
		30.20	509.46
		30.76	537.80
		28.94	591.44
		30.44	651.10
		30.85	703.84
2	neon	32.18	303.75
		32.25	335.06
		31.78	362.70
		31.72	396.02
		31.11	427.55

Table 4. (Continued)

Run No.	Gas	V_N(cc)	T(^oK)
2	neon	31.44	481.34
		30.49	537.16
3	neon	31.48	321.79
		30.96	355.37
		26.73	389.05
		31.89	428.51
		31.71	468.96
		31.22	484.80
		27.96	516.20
		31.80	543.82
		32.58	578.78
		30.87	602.76

Table 5. $-\beta A$ as a function of temperature

Run No.	Gas	V_R-V_N(cc)	T(^oK)
1	nitrogen	7.463	591.460
		9.251	537.794
		11.199	509.464
		13.521	482.651
		16.522	459.429
		19.116	439.022

Table 5. (Continued)

Run No.	Gas	V_R-V_N(cc)	T(^oK)
1	nitrogen	21.544	429.617
		31.727	400.753
		41.437	374.942
		58.722	346.839
1	argon	7.763	591.469
		8.912	537.789
		12.083	509.467
		13.687	482.672
		16.954	459.424
		19.575	439.016
		20.765	429.625
		29.019	400.753
		37.729	374.925
		52.786	346.852
1	carbon monoxide	9.792	591.468
		11.314	537.773
		14.646	509.473
		17.920	482.683
		22.992	459.420
		27.063	439.004
		29.368	429.641
		41.366	400.753
		57.122	374.913
		81.952	346.873
1	methane	15.916	591.468
		23.905	537.758

Table 5. (Continued)

Run No.	Gas	$V_R - V_N$(cc)	T(^{o}K)
1	methane	30.816	509.476
		39.496	482.696
		50.031	459.412
		61.870	439.005
		68.745	429.652
		101.210	400.755
		149.010	374.902
		230.000	346.914
1	ethane	45.924	651.140
		79.807	591.460
		137.570	537.735
		195.150	509.480
		282.800	482.732
		407.020	459.413
		579.030	439.034
		691.990	429.668
1	ethylene	25.258	703.771
		37.146	651.130
		63.092	591.467
		104.220	537.745
		144.500	509.479
		202.820	482.713
		286.000	459.408
		399.680	439.016
		468.940	429.672
1	propane	88.988	703.764

Table 5. (Continued)

Run No.	Gas	V_R-V_N(cc)	T($^\circ$K)
1	propane	147.700	651.154
		294.861	591.451
		614.336	537.735
2	nitrogen	11.450	537.166
		15.440	481.330
		25.600	427.545
		35.160	396.003
		52.320	362.702
		79.970	335.074
		135.730	303.774
2	argon	10.750	537.171
		14.820	481.322
		25.220	427.541
		33.380	395.998
		49.200	362.709
		70.300	335.078
		118.880	303.798
2	carbon monoxide	14.030	537.169
		21.230	481.321
		34.950	427.536
		47.800	395.992
		74.090	362.711
		112.220	335.088
		205.900	303.830
2	methane	45.260	481.320
		79.580	427.530

Table 5. (Continued)

Run No.	Gas	V_R-V_N(cc)	T(^oK)
2	methane	118.770	395.994
		201.670	362.723
		336.470	335.104
3	argon	15.033	484.813
		22.856	428.489
		36.900	389.053
		48.564	355.363
		80.418	321.783
3	nitrogen	15.417	484.815
		21.566	428.490
		36.743	389.061
		52.872	355.357
		91.182	321.769
3	carbon monoxide	19.940	484.823
		32.642	428.496
		54.320	389.058
		78.913	355.344
		137.202	321.770
3	methane	15.396	602.736
		38.861	484.830
		73.138	428.486
		126.687	389.051
		216.839	355.550
		426.522	321.782
3	ethylene	57.600	602.728
		70.398	578.779

Table 5. (Continued)

Run No.	Gas	V_R-V_N(cc)	T($^{\circ}$K)
3	ethylene	101.737	543.791
		142.679	516.190
		205.973	484.847
		259.523	468.953
		494.301	428.495
3	ethane	71.680	602.731
		89.411	578.774
		131.900	543.783
		189.140	516.175
		281.573	484.860
		360.686	468.935
3	propylene	230.416	602.731
		304.517	578.766
		501.807	543.784
		786.787	516.158
3	propane	257.944	602.724
		346.928	578.756
		577.854	543.782